AERODYNAMIC STABILITY OF SUSPENSION BRIDGE SECTION MODELS

by

WILLIAM J. HAYDUK

Thesis submitted to the Graduate Faculty of the
Virginia Polytechnic Institute
in candidacy for the degree of

MASTER OF SCIENCE
in
Applied Mechanics

APPROVED:

Director of Graduate Studies

Dean of Engineering

APPROVED:

Head of Department

Major Professor

September, 1955
Blacksburg, Virginia

TABLE OF CONTENTS

I. LIST OF FIGURES

II. SYMBOLS

A	Area of the Deck (Center to Center of Girders)
C_D	Coefficient of Drag
C_L	Coefficient of Lift
C_M	Coefficient of Moment
C.P.	Center of Pressure
D	Drag Force
F_o, P	Force Amplitude
F	Harmonic Force
F_1, F_4	Phase Difference Correction Factors, Found by Integrating the Effect of Pressure Distribution Across the Section
G_2	Phase Difference Correction Factor , Found in the Same Way as F_1 and F_4
I	Mass Moment of Inertia per Unit Length of Structure
L	Lift Force
N, n	Frequency of Vibration
R	Reynolds' Number
R_1	Resultant of Lift and Drag Forces
S_1	Slope of the Static Lift Curve for the Straight Model
S_2	Slope of the Static Torque Curve for the Straight Model
S_4	Slope of the Static Torque Curve for the Curved Model
V	Velocity

X', X'', X_o, a	Amplitudes
W	Work
a_o	Steady State Amplitude
a_1	Four Times the Radius of Gyration Squared Divided by the Square of the Chord Width
b	Chord Width
c	Fin Width
d	Depth of the Section
e	Eccentricity
h	Lateral Spacing of Vortex Rows
k	Elastic Spring Constant
l	Spacing of Vortices a Short Distance Behind Plate
m	Mass
$\underline{n}$	Number of Test
r	Damping Coefficient
r_c	Critical Damping Coefficient
s	Slot Width
t	Time
$u, \frac{\rho b^2}{m}$	Mass Density Ratio
x	Displacement
α	Angle of Attack
β	Angle of Incidence
$\delta, \delta_a, \delta_n, \delta_s$	Logarithmic Decrements
ρ	Density of Air

ϕ	Phase Angle
ω	Angular Velocity
ω_n	Natural Frequency

III. INTRODUCTION

The problem of aerodynamic instability of flexible bridge spans is one that has faced the engineering profession for many years. Only recently, however, have there been any systematic attacks made on the solution of the problem and methods proposed for removing the cause of the difficulty. Research programs have been undertaken at various colleges and universities throughout the country to study the aerodynamic stability characteristics of models of actual suspension bridges and of simple deck or roadway sections by wind tunnel tests. Much information has been obtained from these test programs which has removed some of the air of mystery surrounding the problem. The present investigation contains the results of one of these test programs which has been conducted at the Virginia Polytechnic Institute.

One important criterion that has been confirmed as a result of these investigations is the fact that the response of a suspension bridge to wind is a function of the shape of the deck or roadway. Therefore, it is important to discover and evaluate aerodynamically favorable arrangements of the structural elements in the deck, in order to remove the cause of the instability. With

this view in mind, the first objective of this thesis is to investigate the stability characteristics of five promising deck sections by wind tunnel tests on models of various depth and width ratios, various size deck openings and various fin widths. The aerodynamic characteristics of a section are obtained from two types of tests: static and dynamic. Static testing involves measurement of components of the force exerted by moving air on a model that is not free to move. Dynamic testing involves determination of the response of an elastically mounted model to the effects of a range of wind speeds.

In previous studies certain discrepancies were found to exist between theoretical and experimental results. Since the theory was based on the assumption that the oscillations of a suspension bridge were caused by self-excited motion alone, the conclusion was drawn that the difference was probably due to forced motion caused by the Karman effect also being measured experimentally. In an effort to show that a forced motion is the cause for the difference, Dr. Steinman has developed an expression for the determination of aerodynamic stability based upon the excitation of a body by an external harmonic force. The partial substantiation of this expression by

wind tunnel tests on section models is the second objective of this thesis.

The five basic sections that are investigated here were selected as a result of previous investigations conducted at V.P.I. in conjunction with their test program concerning aerodynamic stability of suspension bridge sections[18] (see Bibliography). This investigation is a continuation of this test program and it is hoped that by determining basic bridge sections which are aerodynamically stable, the engineer will be afforded a guide which will enable him to design stable sections more readily.

IV. REVIEW OF LITERATURE

Before entering into a discussion of aerodynamic stability, definitions of the terminology used are presented. In all cases the definitions are those which are currently accepted as standard in the literature on the subject.

A. TERMINOLOGY

1. Aerodynamic Coefficients. The force exerted by a fluid on an immersed body depends upon the relative velocity between the body and the fluid. This resultant force is usually resolved into two components; one in the direction of flow called "drag" and one normal to this direction called "lift"[2]. In general, this resultant force will not act through the center of the body and therefore will cause a "torque" or moment effect[9].

By experiment or dimensional analysis the most convenient form for determining lift, drag and torque has been found to be[2,9]:

$$\text{Lift} = C_L \frac{\rho}{2} V^2 A$$

$$\text{Drag} = C_D \frac{\rho}{2} V^2 A$$

$$\text{Torque} = C_M \frac{\rho}{2} V^2 A b$$

where

C_L, C_D and C_M are dimensionless coefficients depending upon the shape of the cross section and Reynolds Number

A is the area of the deck (center to center of girders) (square feet)

b is the chord or width of the section (feet)

ρ is the density of the air (slugs per cubic foot)

V is the velocity of the air (feet per second)

$\frac{\rho V^2}{2}$ is the dynamic pressure (pounds per square foot)

2. Center of Pressure. The location of the resultant force (R_1) acting on a body is called the "center of pressure" and is important in the study of the forces acting on a basic bridge section. It is standard practice

in aerodynamics and hydrodynamics to express the distance from the center of the section to the center of pressure as a percentage of the chord. By dividing the slope of the torque curve by the slope of the lift curve this percentage known as the eccentricity (e), can be determined. since

$$C_M = \frac{\text{Torque}}{\frac{\rho V^2}{2} Ab} \text{ and } C_L = \frac{\text{Lift}}{\frac{\rho V^2}{2} A}$$

therefore

$$\frac{C_M}{C_L} = \frac{\text{Torque}}{\text{Lift} \times b} = \frac{C.P.}{b} = e$$

where C.P. is the center of pressure measured from the mid-span of the chord[9,17].

3. Forces on Basic Bridge Section. The resultant force is also dependent upon the angle of attack (α). This is the angle measured between the chord of the section and the relative wind direction.

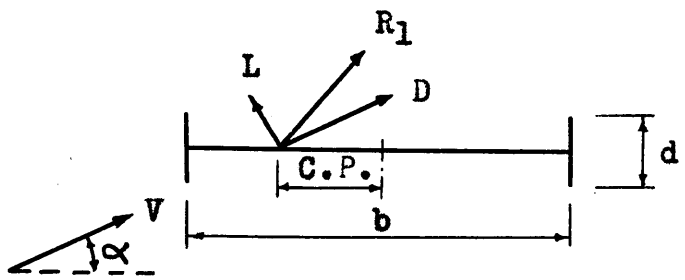

Figure 1. Forces on Basic Bridge Section

4. Logarithmic Decrement (δ). Information obtained from the dynamic tests is presented in terms of the logarithmic decrement. This is defined as the natural logarithm of the ratio of the amplitudes of two successive cycles in an oscillating system[8]. For practical purposes, because of the relatively small values of decrement encountered in these tests, the logarithmic decrement was determined from

$$\delta = \frac{1}{n} \ln \frac{X'}{X''}$$

where n represents the number of cycles required to effect the decay of half the amplitude

X' is some initial amplitude

X" is an amplitude equal to one-half the initial amplitude.

5. Structural Damping. All damping effects, exclusive of aerodynamic factors, are included in structural damping. These effects include internal hysteresis due to varying stress conditions and friction due to relative movement of the elements of the deck[13].

6. Self-excited Vibrations. The alternating force that amplifies and sustains the oscillation is created or controlled by the oscillation itself in a self-excited vibration. Therefore, the alternating force is automatically acting at the natural frequency of the body itself. The oscillations of flexible bridge spans are considered in this category[16].

7. Forced Vibrations. The alternating force that initiates, amplifies and sustains the vibration exists independently of the vibration itself in a forced vibration. This force is present regardless of whether the body upon which it acts is in motion or not. In this case the frequency of the alternating force is independent of the natural frequency of the body and any resonant condition is dependent upon accidental resonance. Vibrations identified with vortex shedding are considered as forced vibrations[16].

8. Section Ratio. In order to apply results obtained from model tests to their prototypes, it is important that several scale relationships be preserved. One such relationship is the ratio of the depth of the girder to the chord or width of the section[1,14].

9. Aspect Ratio. Another important relationship necessary for transferring results from one system to another is the ratio of the span length to the chord or width of the section, called the aspect ratio[1,9]. In these tests end plates were used to obtain essentially two dimensional parallel flow or an aspect ratio of infinity.

10. Mass-Density Ratio. In order to transfer values of the logarithmic decrement from one system to another the mass-density ratio must be used. For vertical motion (dynamic tests) this ratio appears in the form $\frac{\rho b^2}{m}$. For torsional motion (dynamic tests) this ratio appears in the form $\frac{\rho b^4}{8I}$. In these expressions "m" is the mass per unit length of structure, "I" is the mass moment of inertia per unit length of structure, and the other parameters are as previously defined[13]. In all cases the decrement is multiplied by the appropriate mass-density ratio before transferring to another system.

B. AERODYNAMIC STABILITY

1. Stability. The response of a suspension bridge to wind is chiefly a function of the shape of the deck. Basically, then, the problem of aerodynamic instability in flexible bridge spans reduces to the selection of a deck section whose proportions are of a stable character.

From a report by Maher and Becker[13] describing instability, they state:

> "The basic difficulty with the suspension bridge arises from a property described as aerodynamic instability. Fundamentally, this means that a deck section has such a shape that the pressures generated by moving air produce a downward force when the body is moving downward and an upward force when the body is moving upward thus causing increasing amplitudes in each cycle. This effect is continued until a limiting amplitude is reached or the amplitude becomes high enough to cause disintegration of the structure. This situation may occur in vertical or torsional (rocking) motion or in a combination (coupled) motion."

On the other hand, when an aerodynamically stable section, free to oscillate elastically, is given an initial amplitude, it will experience a progressive decay in amplitude because of the forces acting on it.

By idealizing the bridge section into a mass, spring and damper system for vertical motion a clearer concept of instability may be visualized. It is assumed

that a harmonic lift force is acting on the body (mass) at the natural frequency of the system[13]. If the general case of a harmonic force (F) leading the displacement (x) by a phase angle (ϕ) is considered for this idealized system, the displacement and force may be represented as

$$x = X_o \text{ Sin}(\omega t - \phi)$$

$$F = F_o \text{ Sin } \omega t$$

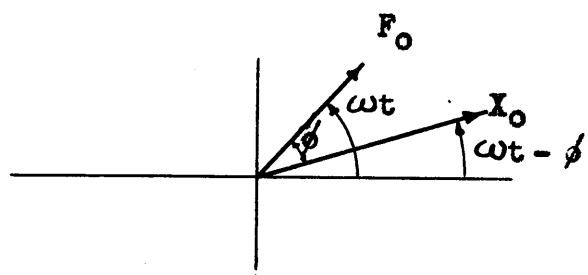

Figure 2. Harmonic Force and Displacement

where "X_o" is the displacement amplitude, "F_o" the force amplitude and "ω" is the angular velocity. The work done per cycle on the system becomes

$$\text{Work} = \pi F_o X_o \text{ Sin } \phi$$

If the energy input is only partially dissipated by the structural damping present, then an unstable condition results. If the energy output to structural damping

exceeds the energy input to the system then a stable condition exists. In the usual structure, this structural damping is rather low, although values in the range of 0.05 to 0.10 have been reported on some actual bridges[7].

The lift force on a vertically oscillating section is a function of the dimensionless parameter V/Nb, where "N" is the frequency, "V" the wind velocity and "b" the chord or width of the deck[13]. In the usual dynamic tests this parameter (V/Nb) is plotted against the logarithmic decrement. Theoretically[19] it has been shown that for certain deck sections, the decrement has alternating positive and negative values approaching a constant value at high values of V/Nb. Depending on whether the section is stable or unstable, this approximate constant value of the decrement will be positive or negative, respectively. It can now be seen why there exist regions of limited stability for basically unstable sections and regions of limited instability for basically stable sections[13]. The one vitally important difference between stable and unstable sections is therefore: "A basically unstable section will have an upper critical range that is unlimited and, therefore, potentially catastrophic"[16].

A general theory in the field of aerodynamic stability was proposed by Dr. D. B. Steinman in the October 1949 Proceedings of the American Society of Civil Engineers. Basically, he wrote the general equations for the aerodynamic forces of lift and torque acting on an oscillating section and equated this to the corresponding expression for the dynamic forces acting on the section. The effects of vertical velocity, angular displacement, angular velocity and angle of incidence are included in the aerodynamic expressions. The parameters representing the aerodynamic characteristics of the section and the coefficients representing the variation of the aerodynamic forces with wind velocity are obtained from static wind tunnel tests on straight and curved models[19]. By determining these coefficients from experimental tests, it is possible to predict the general behavior of any bridge section, regardless of how complex it may be. The equations he arrived at for determining stability were:

for pure vertical motion

$$\delta = -\frac{u}{4}(F_1S_1)\frac{V}{Nb} \quad \text{.... eq. 13 (Dr. Steinman)}$$

for pure torsional motion

$$\delta = - \frac{u}{2a_1} \left(\frac{G_2 S_2}{K} + F_4 S_4\right) \frac{V}{Nb} \text{ .. eq. 16 (Dr. Steinman)}$$

where

δ is the logarithmic decrement

u is the mass-density ratio $(\frac{\rho b^2}{m})$

$\frac{V}{Nb}$ is the velocity ratio

S_1 is the slope of the static lift curve for the straight model

S_2 is the slope of the static torque curve for the straight model

S_4 is the slope of the static torque curve for the curved model

a_1 is four times the radius of gyration squared divided by the square of the chord width

F_1, F_4 and G_2 are correction factors, found by integrating the effect of pressure distribution across the section, to account for the phase difference ... eq. 5 (Dr. Steinman)

2. Criteria for Stability. From static tests on non-oscillating models it is possible to determine criteria for catastrophic instability[13]. Static tests are usually reported as plots of the coefficients of lift,

drag and torque versus angle of attack. If the slope of the lift graph plus the value of the drag coefficient at a particular angle of attack is positive, then the section under test will be vertically stable for high ranges of V/Nb. Similarly, if the slope of the torque graph is positive then the section will be torsionally stable at high ranges of V/Nb. In either case, if negative values result then the section will be catastrophically unstable. For the theoretical proof of these criteria see D. B. Steinman[15] or J. P. Den Hartog[3].

From dynamic tests, which are here reported as plots of the logarithmic decrement versus the parameter V/Nb, it is possible to determine the ranges of stability or instability depending upon whether the sum of the structural damping plus the logarithmic decrement is positive or negative, respectively.

C. VORTEX EFFECT

The classical representation of the Karman vortex effect is shown by a cylinder moving transversely at a uniform velocity through a fluid or by a fluid moving steadily past a stationary immersed cylinder. For this condition, eddies are shed periodically from the cylinder forming the well-known Karman vortex trail. Each time an

eddy is released, an unbalanced lateral force acts on the cylinder. If the cylinder is free to oscillate laterally, then a forced vibration at the eddy frequency may result due to these lateral unbalanced forces. Should the natural frequency of the cylinder be at or near the eddy frequency the vibration of the cylinder may reach a large amplitude[16].

It is believed that a similar effect occurs on deck sections caused by alternating flow around the girders, particularly around the edges of the leading girder. The usual bridge section is composed chiefly of essentially flat members with relatively sharp edges, therefore, it is significant to note the findings made by Fage and Johansen[4] in their study of the wake behind a flat plate of infinite span (1927). These experiments indicated that for the vortex trail behind the plate $1/d \sin\beta$ remained substantially constant (equal to 5.32 average) as the angle of incidence varied between 30° and 90°. (See Figure 3).

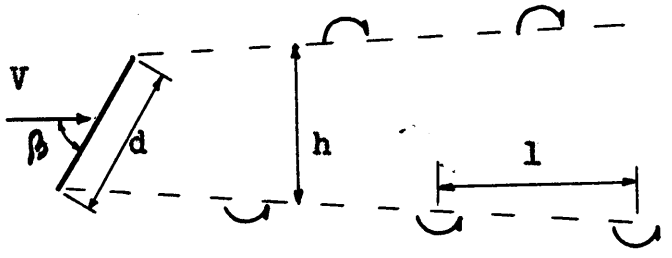

Figure 3. Vortex Trail Behind Infinite Flat Plate

where

V is the velocity in undisturbed air relative to plate

d is the depth of plate (which had knife sharp edges)

h is the lateral spacing of vortex rows

l is the spacing of vortices a short distance behind the plate

β is the angle of incidence of plate

The usual range of angles of attack for static tests is -15° to +15° which would correspond to Fage and Johansen's angle of incidence range of 75° to 90°. They also found that the wake opened out with increasing distance from the plate contrary to von Karman's assumption that "h" remains constant. However, they agree with von Karman's

theoretical value for the ratio h/l = 0.280 at six times the depth of the plate downstream[5]. Another important finding in this investigation was the disclosure that there was a variation in vortex frequency (f) with a change in β. As β was increased from 30° to 90°, f decreased from 0.840 $\frac{V}{I}$ to 0.766 $\frac{V}{I}$. For a more complete study of the role of the vortex in aerodynamic excitation of suspension bridges see Farquharson[5].

In 1941, Dr. Steinman advanced the possibility of the vortex effect having contributed to the failure of the Tacoma Narrows Bridge. Because of space limitation a portion of a paper written by Dr. Steinman, which was subsequently published, was omitted ("The Rigidity and Aerodynamic Stability of Suspension Bridges" American Society of Civil Engineers, 1943). Concerning the reasons why the Tacoma Bridge failed, the following is part of the omitted portion of that paper[20].

The existing theory does not explain .....

> "1. Why the lower (and more dangerous) modes did not appear at the <u>higher</u> wind velocities (as they have appeared on other bridges; and
>
> "2. Why each mode had a <u>most favorable wind velocity</u>, apparently definitely related to the oscillation frequency. This relation followed a law that was too regular to be accidental.

"The preceding analysis based on aerodynamic instability therefore needs to be supplemented or modified for a more complete solution of the problem. To supply a physical answer to these remaining questions, two alternative (and possibly related) explanations are offered:

"1. The Von Karman vortex effect.

"2. A low-velocity effect whereby aerodynamic instability is created by the phase difference (relative to wind velocity) across the width of the section. (This relation, as applied to vertical oscillations, has hitherto been unsuspected and unexplored.)

The Von Karman Vortex Effect

"The vortex theory requires resonance of the oscillations with the vertical impulses of automatically generated alternating vortices whose frequency depends on the wind velocity. The established relation is of the form(3)

$$N \approx 0.22 \frac{V}{d} \quad \ldots\ldots\ldots \quad (40)$$

where d usually denotes the diameter of a circular section but is here tentatively applied to the girder depth of a bridge cross-section. This would explain the selective determination of mode of oscillation as a function of wind velocity, if the Von Karman effect is active in creating, modifying or amplifying the initial oscillations. The recorded values of most favorable wind velocities for the different modes on the Tacoma span are very closely checked by the above formula with a slight modification, namely an indicated reduction in the numerical coefficient at higher velocities:

$$N \approx \frac{V}{d} \left(.234 - \frac{V}{350}\right) \quad \ldots \quad (40a)$$

where all units are in feet and seconds. (The factor 350 presumably includes some velocity constant to balance the dimensions.) The comparison is as follows:

n	N/minute	V (by Eq. 40a)	Observed Most Favorable V
1	8	3.3 MPH	3.3 MPH
3	12	5.1	5
4	16.5	7.4	7.5
5	21	9.9	10
6	24	11.8	12
7	27	13.9	14

Where sufficient observations were available, the frequencies of other observed wind velocities were distributed around the respective most favorable velocities in the general form of a probability curve.

"The Von Karman vortex effect is generally identified with aerodynamically stable sections. Some intermediate or border-line cross-sections may also be subject to this action. The successive or combined action of resonant vortices and aerodynamic instability might explain the behavior of the Tacoma span.

"The official report on the Tacoma bridge failure (by a board of engineers consisting of O. H. Ammann, M. Am. Soc. C. E., Theodor Von Karman, M. Am. Soc. C. E., and Glenn B. Woodruff, M. Am. Soc. C. E.) discarded the vortex effect as an explanation of the vertical oscillations, principally because the required sharp correlation between wind velocity and oscillation frequency was lacking.

"Oscillations observed on other bridges closely check the analysis based on aerodynamic instability, and are fully explained thereby, without involving any indicated influence of the Von Karman effect."

In 1942 a report by Farquharson and Dunn[6] indicated rather definitely that the probable cause of bending oscillations in the Tacoma Narrows Bridge were a result of vortex shedding. In 1943 a report by Von Karman and Dunn[10] on the investigation of this same bridge stated, in part,

> "Resonance between the frequency of vortex shedding and one of the natural frequencies of the bridge (Tacoma Narrows) was often suggested as the reason for the vertical oscillations. However, this hypothesis does not explain the fact that self-excited oscillations exist over rather wide ranges of velocities. It has been found that in general the vortex frequency produced by a blunt obstacle in the wind stream is proportional to the wind velocity. Hence, clear cut resonance could exist only at well defined wind velocities. It appears that the phenomenon is determined by the following conditions:
>
> a) While the structure is at rest the vortex frequency is controlled by the wind.
>
> b) At certain discrete wind velocities, which we will designate as the "critical velocities," the vortex frequency will either coincide with, or be a multiple of, one of the frequencies of motion of the structure. Such coincidence results in self-excited oscillations.
>
> c) Beyond the critical wind velocities the oscillating structure and not the wind velocity controls the vortex frequency. In such cases the range of oscillation extends over certain finite ranges of wind velocity. The lower limit of each range is a critical velocity. The upper limit is not as well defined as the critical velocity. However, between the upper limit and the next critical velocity the structure is practically at rest."

In 1947 Dr. Steinman stated[16]

> "In the past, two categories of instability problems have been distinguished: self-excited vibrations, and forced vibrations.
>
> "Recent discoveries tend to efface the line of demarcation between these two classifications of instability problems. It has been found that vibrations identified with vortex shedding also involve automatic synchronism, or control of impulse frequency by vibration frequency, once the vibrations have been initiated. This broadens the base of similarity and correspondence between the two types of instability and strengthens the prospect of ultimately reducing all instability phenomena to a common basic explanation and analysis."

In 1955 a report by Maher and Becker[13] showed discrepancies existing between the theory proposed by Dr. Steinman[19] and experimental results from dynamic tests on section models. There was disagreement with respect to the scale of the decrement values and with respect to the location of critical values of V/Nb. However, there was agreement in the overall form of the graphs and in the predicted cycling of the stable and unstable regions. Dr. Steinman advanced the explanation for this difference in a supplement to the report[13] which, in part, read

> "The plotted graphs of vertical and torsional stability response presented by Maher and Becker show sharp peaks of limited stability and instability at certain critical velocity ratios. These peaks represent typical resonance effects, superimposed upon the general basic curves given by the writer's theory. The

peak resonance effects represent forced vibrations (due to a harmonic force of independent frequency), whereas the smoother general curve given by the writer's theory represents self-excited vibrations, due to harmonic forces having automatically the frequency of the oscillating section.

"The forced vibrations, producing the peak resonance effects, are similar to those acting on a circular section, and correspond to the shedding of alternate vortices at the top and bottom of the section. (See Reference 16.)

"The superimposed resonance effect (or "vortex effect") appears in a sharply narrow range of low velocity ratio, and is non-catastrophic. It is not a factor in coupled oscillations, which appear at relatively high values of V/Nb."

In December 1954, Dr. Steinman[21] developed a relationship for a harmonic force acting on a body in terms of structural damping, natural and actual frequencies, and steady state and arbitrary amplitude. This expression partially shows that the existing discrepancies between experimental and theoretical results are due to a forced vibration effect. The development of this expression in essence is as follows:

The work done per cycle on an oscillating body with damping is

$$\Delta W = \pi P a \sin\phi - \pi r a^2 \omega$$

where

P is an arbitrary external force

a is an arbitrary displacement

ϕ is the phase angle

r is the coefficient for damping

ω is the angular velocity

The potential energy of this system is

$$W = \frac{1}{2}ka^2$$

where k is the elastic spring constant

The net decrement (δ_n) is assumed equal to the difference between the aerodynamic decrement (δ_a) and the structural decrement (δ_s).

Therefore

$$\delta_n = \delta_a - \delta_s \approx \frac{\Delta W}{2W} = \frac{\pi}{ka} (P\sin\phi - r\omega a)$$

For a steady state condition where δ_n is zero

$$\sin\phi = \frac{a_o}{P} r\omega$$

where "a_o" is the steady state amplitude. The vector representation of the steady state condition is as shown in Figure 4.

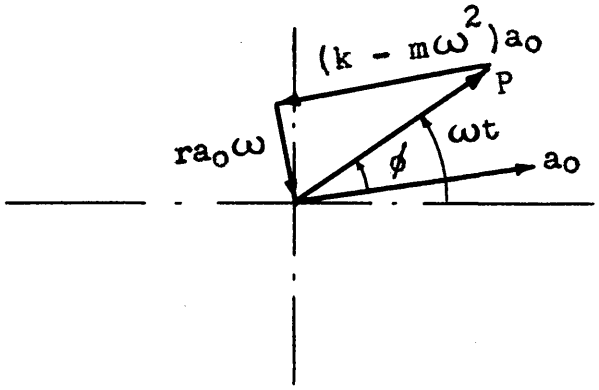

Figure 4. Vector Representation of Steady State Condition

Therefore, the net decrement is

$$\delta_n = \frac{\pi}{ka}(a_o r\omega - ar\omega) = \frac{\pi r\omega}{k}\left(\frac{a_o - a}{a}\right)$$

It is now convenient to put $\frac{\pi r\omega}{k}$ in the following form, where the structural damping is assumed to be viscous. For critical damping

$$r_c = \frac{2k}{\omega_n} \qquad \text{or} \qquad k = \frac{r_c\omega_n}{2}$$

Substituting for "k" $\qquad \frac{\pi r\omega}{k} = \frac{2\pi r\omega}{r_c\omega_n}$

Since $\delta_s = 2\pi\frac{r}{r_c}$ therefore $\frac{\pi r \omega}{k} = \delta_s \cdot \frac{\omega}{\omega_n}$

where

r_c is the critical damping coefficient

m is the mass of the body

ω_n is the natural frequency of the body

Substituting this relation in the previous expression for δ_n it can be seen that

$$\delta_n = \delta_a - \delta_s = \delta_s \cdot \frac{\omega}{\omega_n}\left(\frac{a_o - a}{a}\right)$$

From this it is evident that the following is true: when

$a = a_o$	then	$\delta_a = \delta_s$
$a = 0$	then	$\delta_a = \infty$
$a > a_o$	then	$\delta_a - \delta_s < 0$ (stability)

It should be noted that in <u>this</u> development <u>only</u>, a negative net decrement indicates a <u>stable</u> condition. In all other cases in this thesis a <u>positive</u> decrement indicates <u>stability</u>.

Since the phase angle itself is a variable, except for a steady state condition, this relationship is a

good approximation only for amplitudes relatively close to the steady state amplitude.

V. EXPERIMENTAL INVESTIGATIONS

A. OBJECTIVES

The primary objective of this thesis is to investigate the aerodynamic stability characteristics of five promising basic suspension bridge deck sections. The selection of these five different arrangements of the structural elements in the deck is the result of a test program which has been conducted at V.P.I.[14,18]. Previous static tests on models of similar proportions indicate that the sections presently under investigation will be basically aerodynamically stable. Present static tests have been run to check the stability characteristics of these five particular sections. Dynamic tests have been conducted in order to determine the stability response of these sections to uncoupled torsional and vertical motion, thereby presenting a more complete picture of their aerodynamic stability characteristics.

A second objective of this thesis is to substantiate in part the theory proposed by Dr. Steinman[20], that the present discrepancies existing between experimental and theoretical results, concerning the aerodynamic stability of suspension bridge deck sections, are due to

a forced motion (Karman) effect. Previously, the theory[19] considered only the effect of self-excited motion acting on the section, without any consideration of a forced motion. From a study of dynamic tests run at varying initial amplitudes on a basic H-section, a partial confirmation of this theory of the Karman effect has been presented. A number of unsuccessful attempts were made during this investigation to measure directly the effect of the forced motion by experimental methods. Because of time limitations the completion of this portion of the test program was postponed until a later date. It is believed that in the near future this will successfully be accomplished by using an experimental technique now being developed as part of the continuation of this test program.

B. PLAN OF INVESTIGATION

The plan of investigation was divided into the following three parts: (A) to determine the lift, drag and torque graphs from static tests for the five section models under consideration; (B) to determine the stability response graphs for these same five sections in both vertical and torsional motion; and (C) to

determine the stability response graphs for an H-section in both vertical and torsional motion for various initial amplitudes.

The sections tested are the following variations of girder H-sections: (In all cases the models were 18 inches long and the chord (b) was 8 inches.)

1. Section "a"

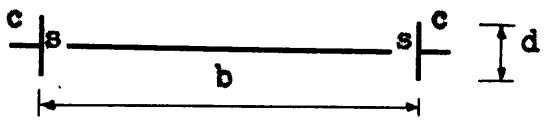

where d/b = 0.15 and c = s = d/2

2. Section "b"

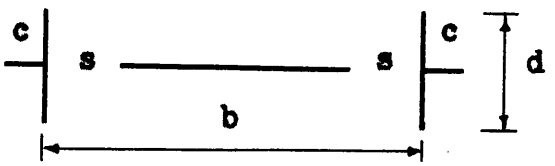

where d/b = 0.30; s = 2/3 d and c = d/4

3. Section "c"

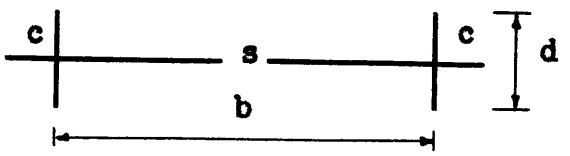

where d/b = 0.26 and c = s = d/2

4. Section "d"

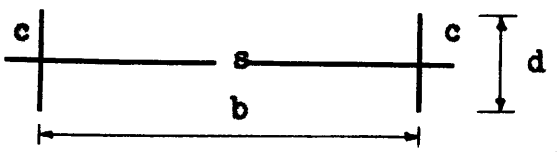

where d/b = 0.26 and c = s = d/3

5. Section "e"

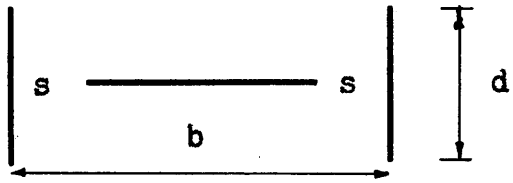

where d/b = 0.38 and s = d/2

6. Girder H-section with d/b = 0.20

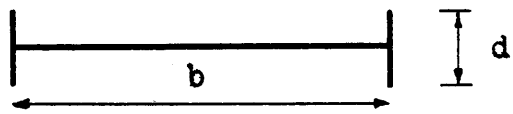

C. APPARATUS AND MATERIALS

1. The models used in this investigation were constructed of an aluminum deck, and detachable aluminum girders and fins. The slots in the deck were open 83-1/3% in the longitudinal direction; the remaining solid portion being required for support of the girders and fins. The width of the slots was varied by inserting appropriate balsa wood plugs which were scotch-taped to the deck. End plates were used to obtain essentially two dimensional flow or an aspect ratio of infinity.

2. The wind tunnel at the Virginia Polytechnic Institute was used for all testing. This tunnel has a 35-horsepower D.C. motor capable of producing wind velocities up to 150 miles per hour. It is a horizontal single return type of tunnel with a three-foot circular open section.

3. The wind velocity was measured with an Alnor Anemometer (hot wire) for speeds up to 600 feet per minute and above this velocity a micromanometer, connected to two static tubes in the tunnel, was used.

4. The static tests were conducted with the model being held in the aluminum frame shown in Figure 5. A top and bottom floor system was used to prevent downwash or upwash from striking the frame. The frame is connected by linkages to a four-component type of balance system which measures lift, drag and torque with an accuracy up to 1/100 of a pound. The angle of attack was measured by means of a circular protractor connected to the model, using a stationary pointer on the frame for reference.

5. The dynamic tests were of two types: vertical motion and torsional motion.

The setup for vertical motion is shown in Figure 6. The steel frame with model and end plates rigidly connected is free to oscillate in a vertical plane only. This is accomplished by means of the four steel bar springs shown rigidly connected to the wooden frame by means of steel mounting blocks. The steel frame is guyed laterally to prevent motion in that direction.

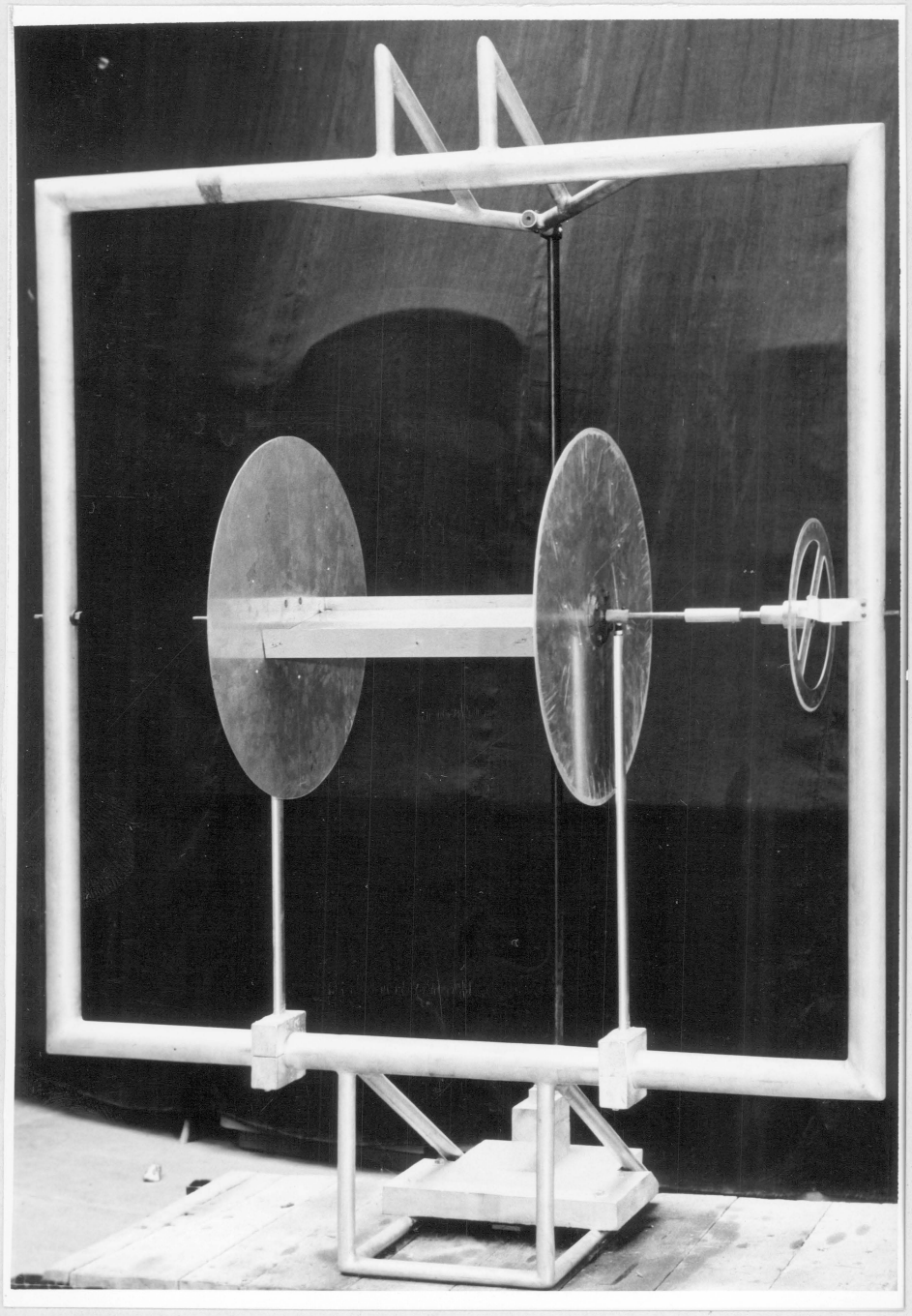

[Photo through courtesy of L. A. Becker(1)]

Figure 5. Static Test Setup

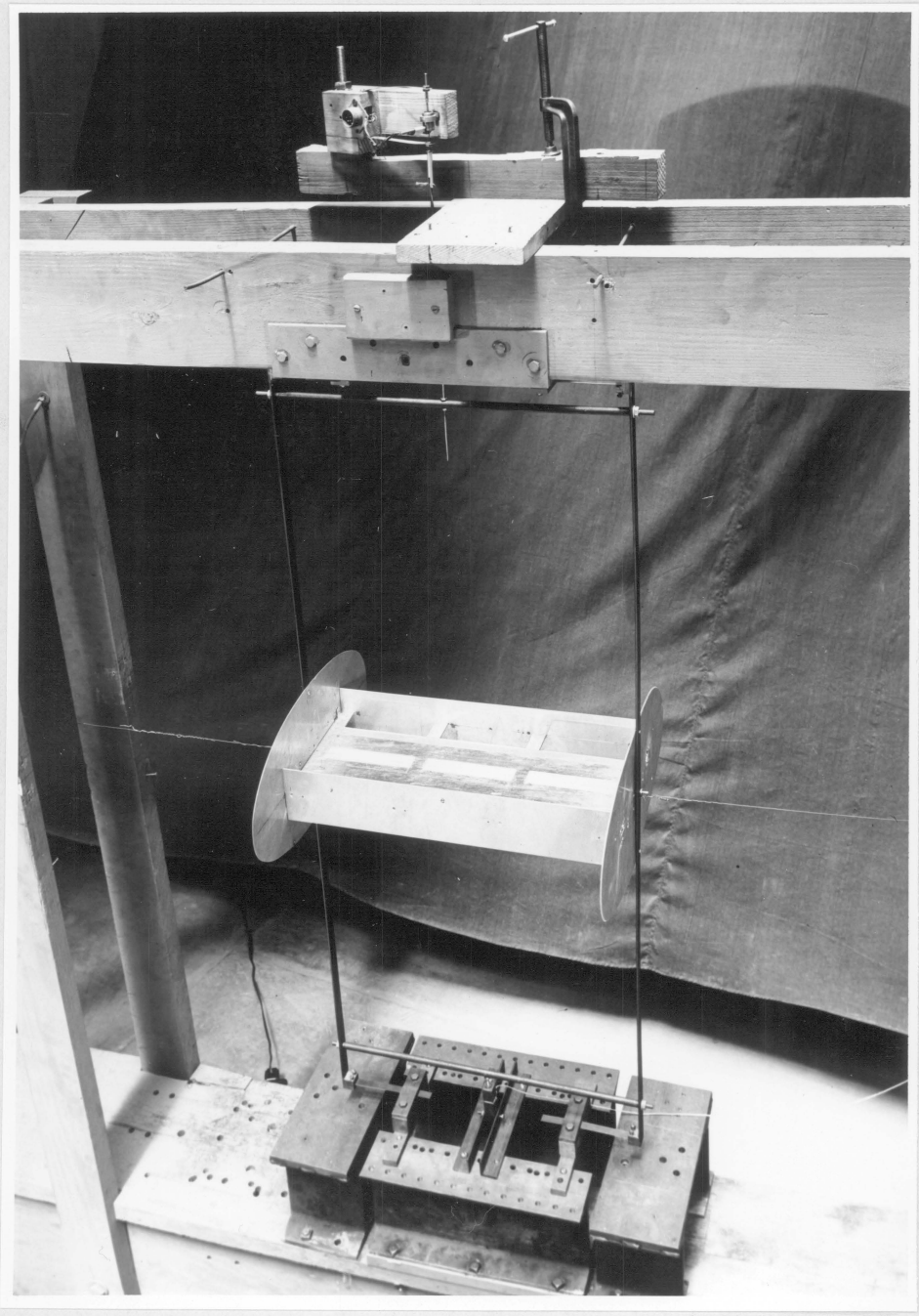

Figure 6. Vertical Motion Setup

The setup for torsional motion is shown in Figure 7. The model is supported by a short shaft at each end which passes through a ball-bearing mount supported by a vertical strut rigidly connected to the frame. The end plates are connected to the ball-bearing mounts and are stationary. The end of each shaft is connected to a steel bar spring held rigidly to the wooden frame allowing the model to oscillate torsionally only.

The oscillations of the model in both types of tests are picked up by a linear variable differential transformer (LVDT), consisting of a coil form and a movable iron core. The core of the LVDT was connected by a linkage to the top of the steel frame for vertical motion (Figure 6) and to the rear fin of the model itself for torsional motion (Figure 7). The relative movement between the coil (which was rigidly connected to the frame) and the core causes changes in inductance in the circuit, which are directly proportional to displacements of the model. The output of the LVDT is fed to a Dyna-Myke which amplifies the signal and in turn feeds it to a Brush Oscillograph which makes a permanent time-displacement record. Since the speed of the moving tape on the Brush Oscillograph is known, the frequency of vibration can be determined easily. By means of this time-

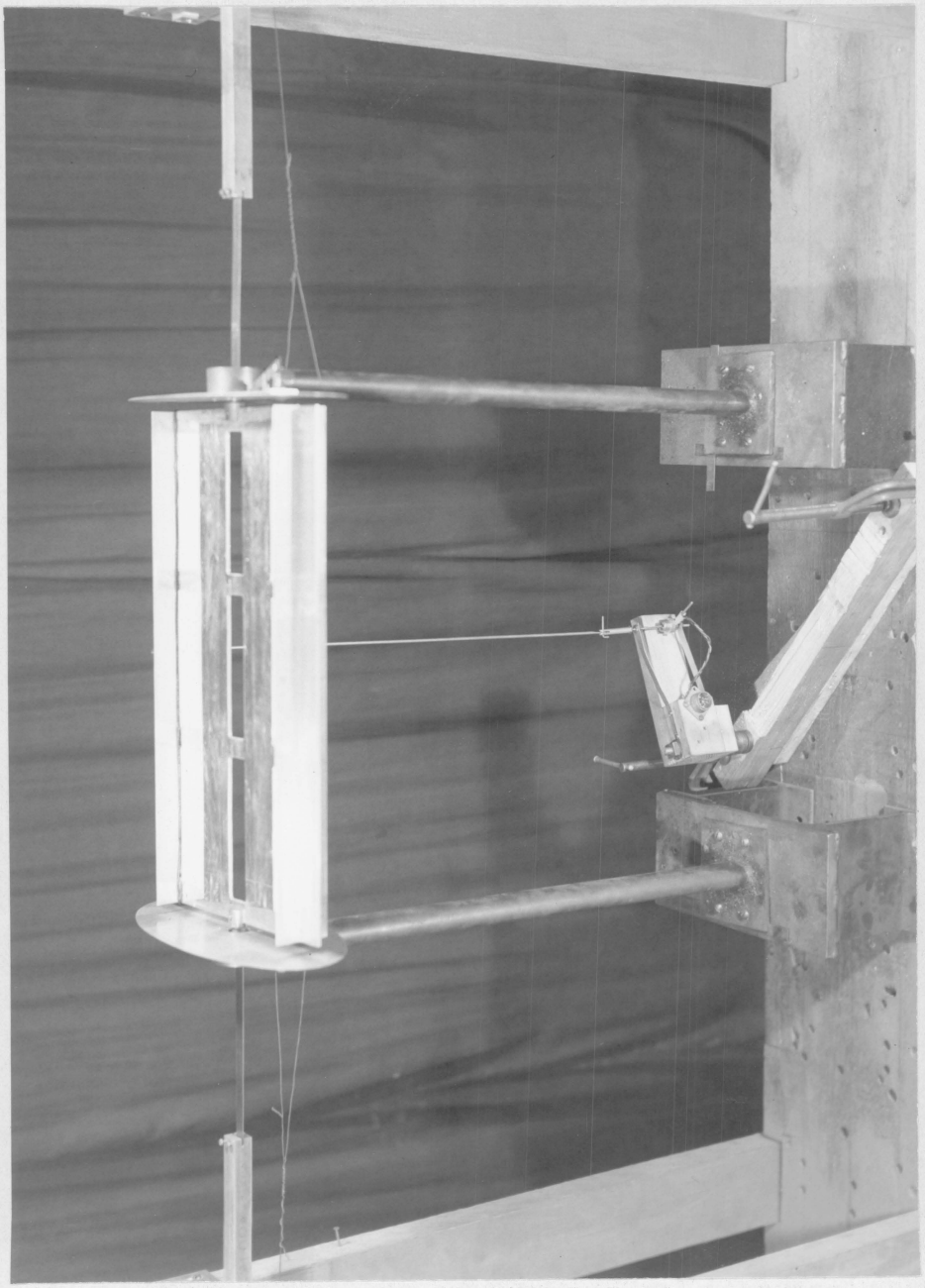

Figure 7. Torsional Motion Setup

displacement record, the logarithmic decrement is also determined by means of the relationship previously noted under "Terminology".

A picture of the entire setup for torsional motion is shown in Figure 8. On the table at the bottom left is the Brush Oscillograph flanked on either side by a Dyna-Myke. The coil of the LVDT is connected to a wooden block which is clamped to the base of the main wooden frame in the tunnel, immediately below the right fin of the model. The movable core of the LVDT is connected to the brass rod extending down from this same fin (trailing edge). The Alnor Anemometer is shown on a shelf on the wooden frame. At the bottom right is shown the micromanometer and the variable resistors which control the speed of the air stream in the tunnel.

For a more complete treatment of the apparatus in the V.P.I. Wind Tunnel see References[1,13,14].

Figure 8. Wind Tunnel with Model Mounted for Torsional Motion, Including Frame and Recording Equipment

D. METHOD OF PROCEDURE

The method of procedure used here is one that has been developed over a period of years and has now become practically standard for static and dynamic tests conducted in the V.P.I. wind tunnel.[14]

1. Static Tests

a. Determination of Tare. The model was removed from the frame and the tare of the frame, end plates and struts was determined by measuring the amount of lift, drag and torque acting at test speed.

b. Dynamic Pressure. All static tests were run at a constant actual dynamic pressure ($\frac{\rho V^2}{2}$) of 2.67 inches of water. By using a constant pressure, the errors due to changes in density and temperature are eliminated.

c. Test Procedure. The model was held stationary in the frame shown in Figure 5 throughout the test. At zero velocity the values of lift, drag and torque were read from the scales in the tunnel pit. Then readings were taken at varying angles of attack from -12 degrees to +12 degrees at two degree increments, while holding the test dynamic pressure constant.

2. Dynamic Tests

a. Determination of Tare. The damping that exists in the frame and supports was measured by replacing the model by a flat steel bar of equal weight. By giving this system an initial displacement at zero velocity the logarithmic decrement was determined from the time-displacement record. This correction was then subtracted from the resulting decrement at the various test speeds. The decrement obtained by using the model itself at zero velocity was very nearly the same as when using the steel bar, therefore, it was decided to use the model itself at zero velocity for the only correction to be made on the decrement. The correction procedure using the flat steel bar of equivalent weight was used only for the vertical motion tests of the H-section.

b. Test Procedure. The models were held in the air stream as shown in Figures 6 and 7. The model was displaced by a known amount from its equilibrium position by a trigger mechanism. At the desired velocity the trigger was released allowing the model to oscillate freely. If the amplitudes, recorded on the Brush Oscillograph tape, diminished as time went on, this indicated a section where the aerodynamic plus the structural damping

were positive. For this case the logarithmic decrement was called positive and computed by the previous formula after selecting an initial amplitude near the beginning of each run and counting the number of cycles required to cause the decay of half the amplitude.

If the amplitudes increase after an initial displacement then the model is held in its equilibrium position and then released, allowing it to oscillate freely. The amplitude was allowed to increase until it approached the practical limit of the LVDT. For this case, the aerodynamic plus the structural damping is negative, consequently the decrement obtained from the record of this type of motion is considered negative.

Readings were taken at zero velocity and at higher velocities spaced at convenient intervals until a V/Nb ratio of five was reached. At this point, if the section showed definite stable characteristics, the testing was terminated. However, if the section showed signs of being unstable for higher ranges of V/Nb, tests were run at higher velocities until a definite trend was established either toward stability or instability. In some cases for sections which were exhibiting neutral qualities at rather high V/Nb ratios, the testing was

discontinued when it was felt that the velocities had reached a practical limit as far as the structural strength of the model was concerned.

c. Initial Displacements. For the vertical motion tests, sections "a" to "e" were initially displaced 0.10 inch from the equilibrium position. For the torsional motion tests, sections "a" to "e" were initially displaced 1.0 degree from the equilibrium position. For the girder H-section, vertical motion tests were run for initial displacements of 0.025, 0.050, 0.075 and 0.10 inch. In the torsional motion tests on the girder H-section, initial displacements of 0.025, 0.50, 0.75 and 1.0 degree were used.

d. Angle of attack. In all dynamic tests an angle of attack of 1.5 degrees was used since the wind tunnel produced an air stream inclined upward at this angle on a model held level with reference to the earth's surface.

E. DATA

1. Static Tests

The coefficients for lift, drag and torque were calculated by using the formulas previously presented. These coefficients were then plotted against the corresponding angles of attack. Because of slight discrepancies in the wind tunnel alignment, these plots do not pass through the origin as they should for symmetric sections. Therefore, the following graphic correction was made:[14]

a. For Lift and Torque

   1. The curve obtained from the actual test was traced.
   2. The trace was rotated 180° and matched with the actual curve.
   3. The actual curve was again traced with its axis.
   4. The mean of these two curves and their axes was taken as correct and plotted in this report[1].

b. For Drag

   A similar correction was made except that in Step 2 the trace was turned over instead of rotated[1].

2. Dynamic Tests

The logarithmic decrement was computed for each run and corrected by subtracting the decrement obtained at zero velocity for the particular section. These decrements were then plotted against the corresponding values of V/Nb. In all cases the natural frequency (N) at zero velocity was used for this parameter (V/Nb).

F. RESULTS

The graphs on the following pages represent the results of this investigation.

1. Section "a".

The static tests of section "a", Figure 9, indicate that the section is vertically stable for angles of attack above +2° and below -2°, while between +2° and -2° the section exhibits neutral qualities since the slope of the lift graph is practically zero in this range. The moment graph indicates torsional instability for angles of attack between +2° to +10° and -2° to -10°, while between +2° and -2°, the section again exhibits neutral qualities. Above +10° and below -10° the graph indicates torsional stability.

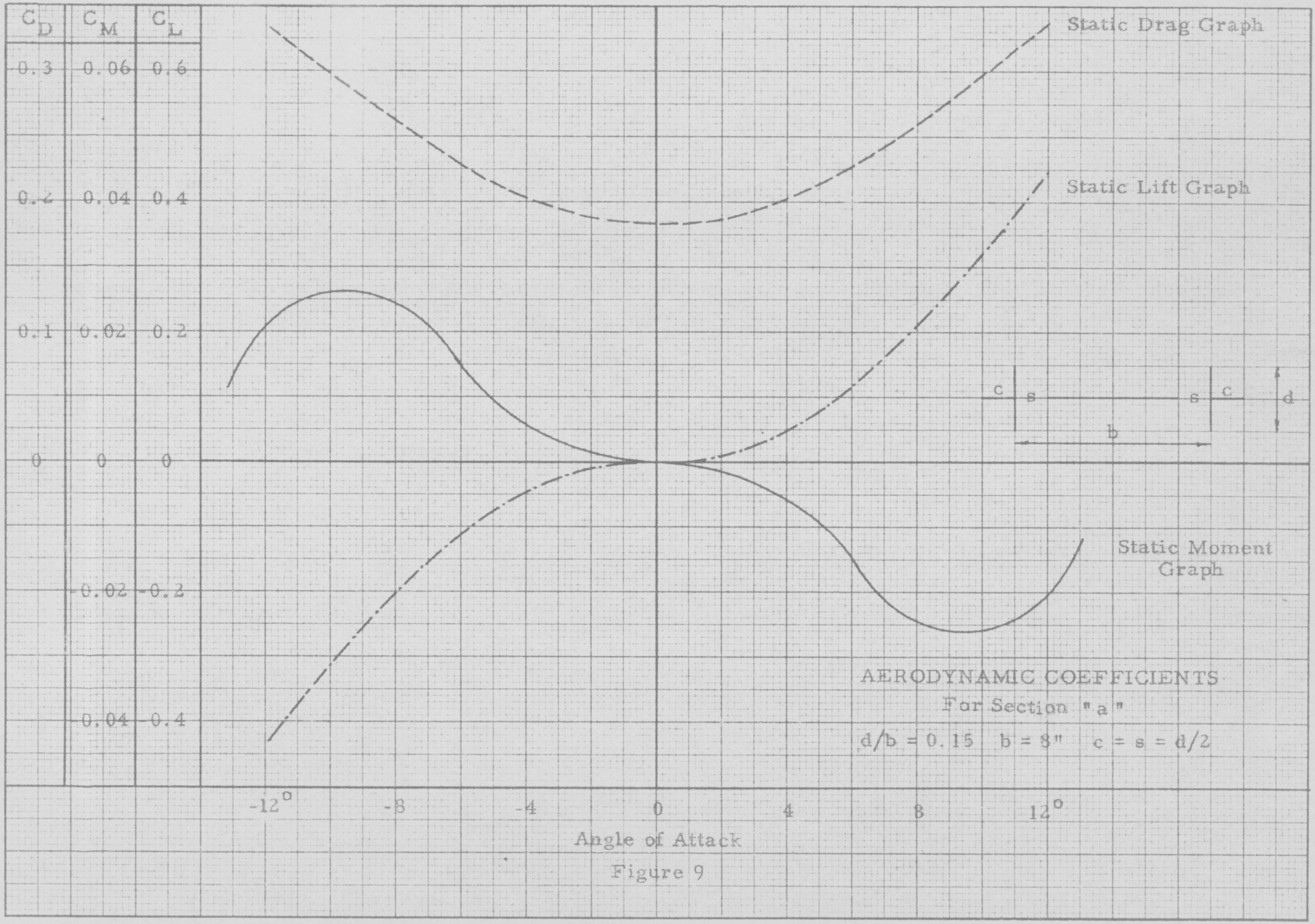
C_D
C_M
C_L
0.3
0.06
0.6
0.2
0.04
0.4
0.1
0.02
0.2
0
0
0
-0.02
-0.2
0.04
0.4
Static Drag Graph
Static Lift Graph
Static Moment Graph
c
s
s
c
d
b
AERODYNAMIC COEFFICIENTS
For Section "a"
d/b = 0.15 b = 8" c = s = d/2
-12°
-8
-4
0
4
8
12°
Angle of Attack

Figure 9

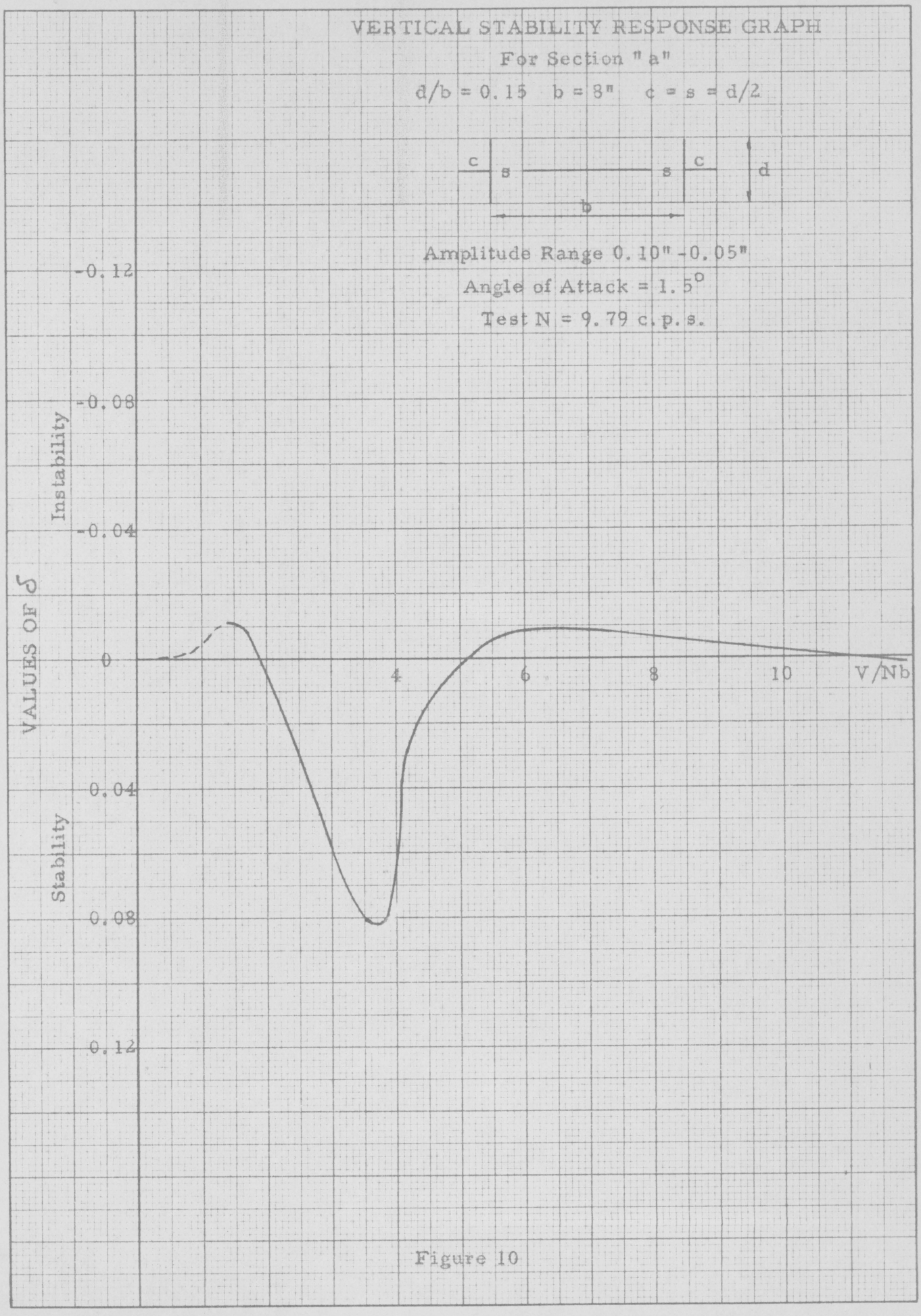
VERTICAL STABILITY RESPONSE GRAPH
For Section "a"
d/b = 0.15 b = 8" c = s = d/2
c
s
s
c
d
b
Amplitude Range 0.10" -0.05"
Angle of Attack = 1.5°
Test N = 9.79 c.p.s.
-0.12
-0.08
-0.04
Instability
VALUES OF δ
0
4
6
8
10
V/Nb
0.04
Stability
0.08
0.12

Figure 10

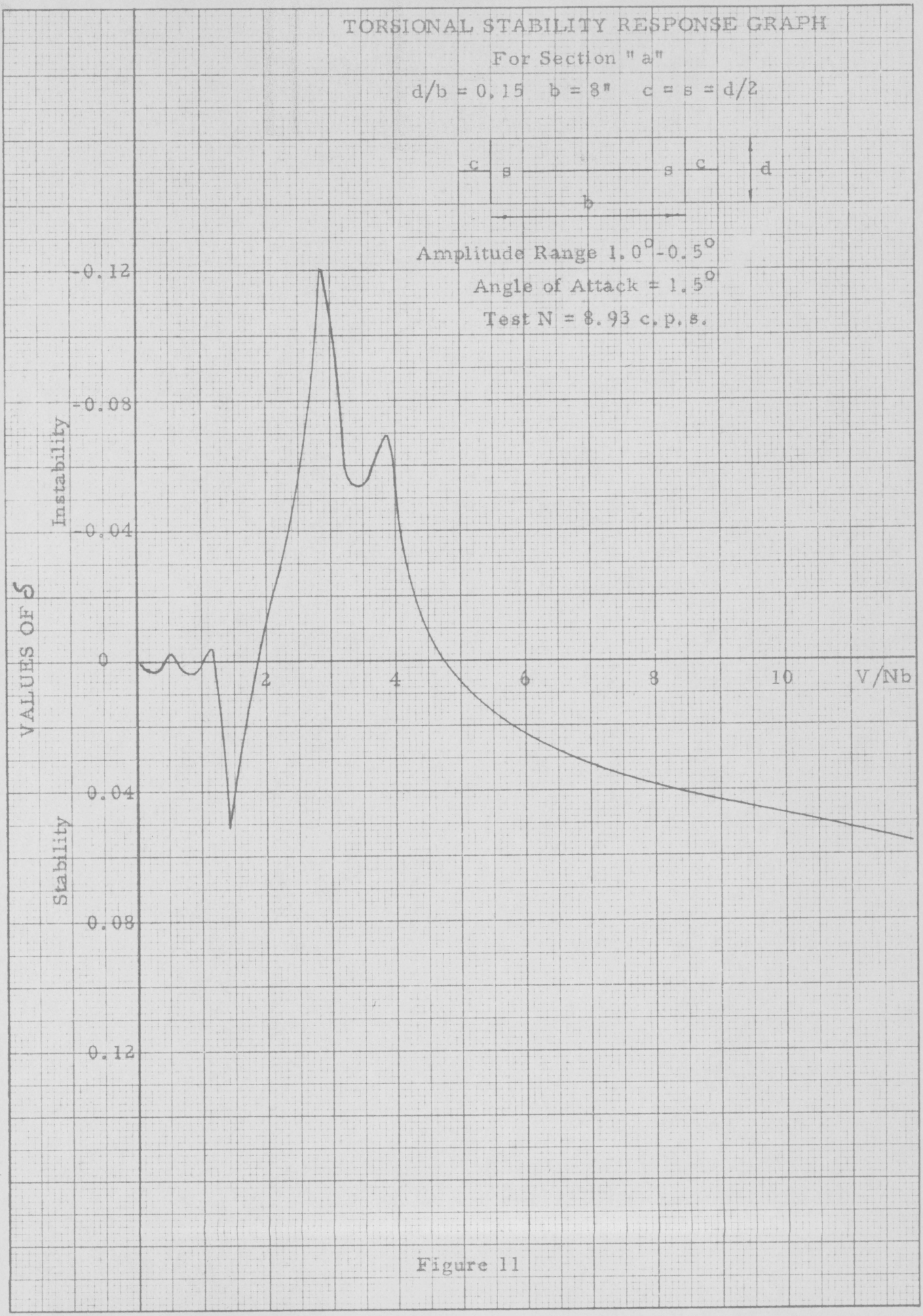
TORSIONAL STABILITY RESPONSE GRAPH
For Section "a"
d/b = 0.15 b = 8" c = s = d/2
c
s
s
c
d
b
Amplitude Range 1.0°-0.5°
Angle of Attack = 1.5°
Test N = 8.93 c.p.s.
VALUES OF δ
Instability
Stability
0.12
0.08
0.04
0
0.04
0.08
0.12
2
4
6
8
10
V/Nb

Figure 11

The dynamic test for the vertical motion of section "a", Figure 10, shows that in the upper critical range, above a velocity ratio (V/Nb) of 5.0, the section is basically neutral although it is very slightly unstable. A relatively small amount of structural damping would shift the axis upward causing this section to be stable. The stable region between velocity ratios of 1.8 and 5.0 presents no difficulty, whereas the limited instability in the second critical range from V/Nb of 0 to 1.8 would also be reduced considerably by structural damping. The torsional stability response graph for this section (Figure 11) indicates torsional stability for velocity ratios above 4.7 and is also stable for all practical purposes from V/Nb of 0 to 1.9. The limited instability condition between velocity ratios of 1.9 and 4.7 might cause uncomfortable vibrations but the inherent damping in the structure would reduce this condition somewhat.

2. Section "b".

This section has the same general shape as section "a", with twice the girder depth, twice the slot width and the same fin width. These changes have improved the torsional stability and at the same time reduced the vertical stability.

The static lift graph for section "b" (Figure 12) indicates vertical instability between angles of attack of -10° and +10°. Outside this range the lift graph indicates a stable region. The static moment graph (Figure 12) indicates a neutral section between -1° and +1° (angle of attack). Between the angles of -1° to -7° and +1° to +7° the section exhibits torsionally stable qualities. Above +7° and below -7° the section indicates instability for torsional motion.

For the dynamic tests above the critical velocity ratio of 3.0 the vertical stability response graph (Figure 13) indicates vertical instability of approximately a constant decrement. If the structural damping were slightly larger than 0.04 this section would be vertically stable for velocity ratios up to at least 12.0. For V/Nb values less than 3.0 the section is vertically stable. The torsional stability response graph of section "b" (Figure 14) indicates a torsionally stable condition above a velocity ratio of 3.0. There is a limited instability condition between velocity ratios of 2.1 and 3.0 which would be reduced somewhat by structural damping. In the V/Nb range between 0 and 2.1 the section indicates torsionally stable characteristics.

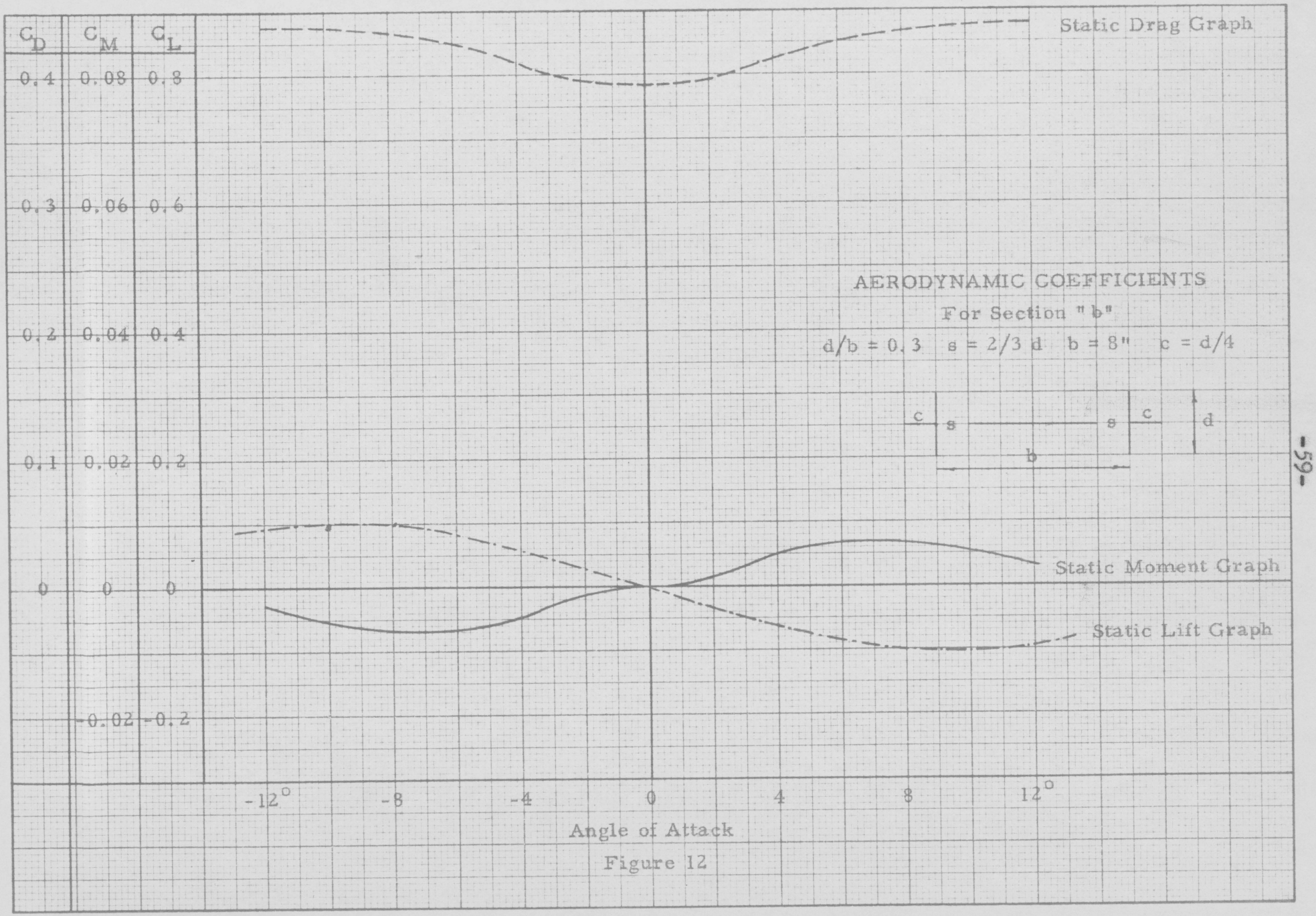
C_D
C_M
C_L
0.4
0.08
0.8
0.3
0.06
0.6
0.2
0.04
0.4
0.1
0.02
0.2
0
0
0
-0.02
-0.2
Static Drag Graph
AERODYNAMIC COEFFICIENTS
For Section "b"
d/b = 0.3 s = 2/3 d b = 8" c = d/4
c
s
s
c
d
b
Static Moment Graph
Static Lift Graph
-12°
-8
-4
0
4
8
12°
Angle of Attack

Figure 12

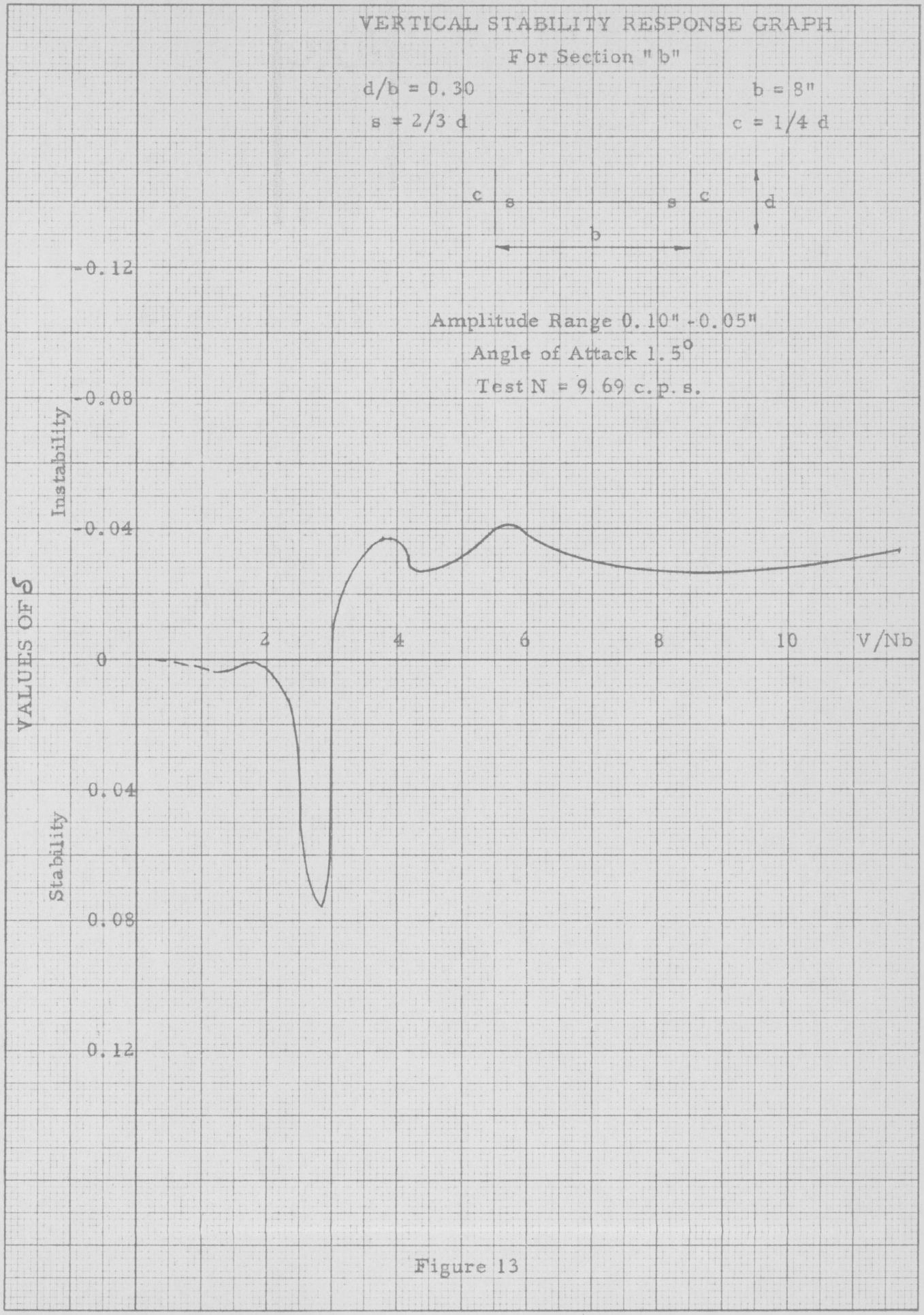
VERTICAL STABILITY RESPONSE GRAPH
For Section "b"
d/b = 0.30
s = 2/3 d
b = 8"
c = 1/4 d
c
s
s
c
d
b
Amplitude Range 0.10" -0.05"
Angle of Attack 1.5°
Test N = 9.69 c.p.s.
VALUES OF δ
Instability
Stability
-0.12
-0.08
-0.04
0
0.04
0.08
0.12
2
4
6
8
10
V/Nb

Figure 13

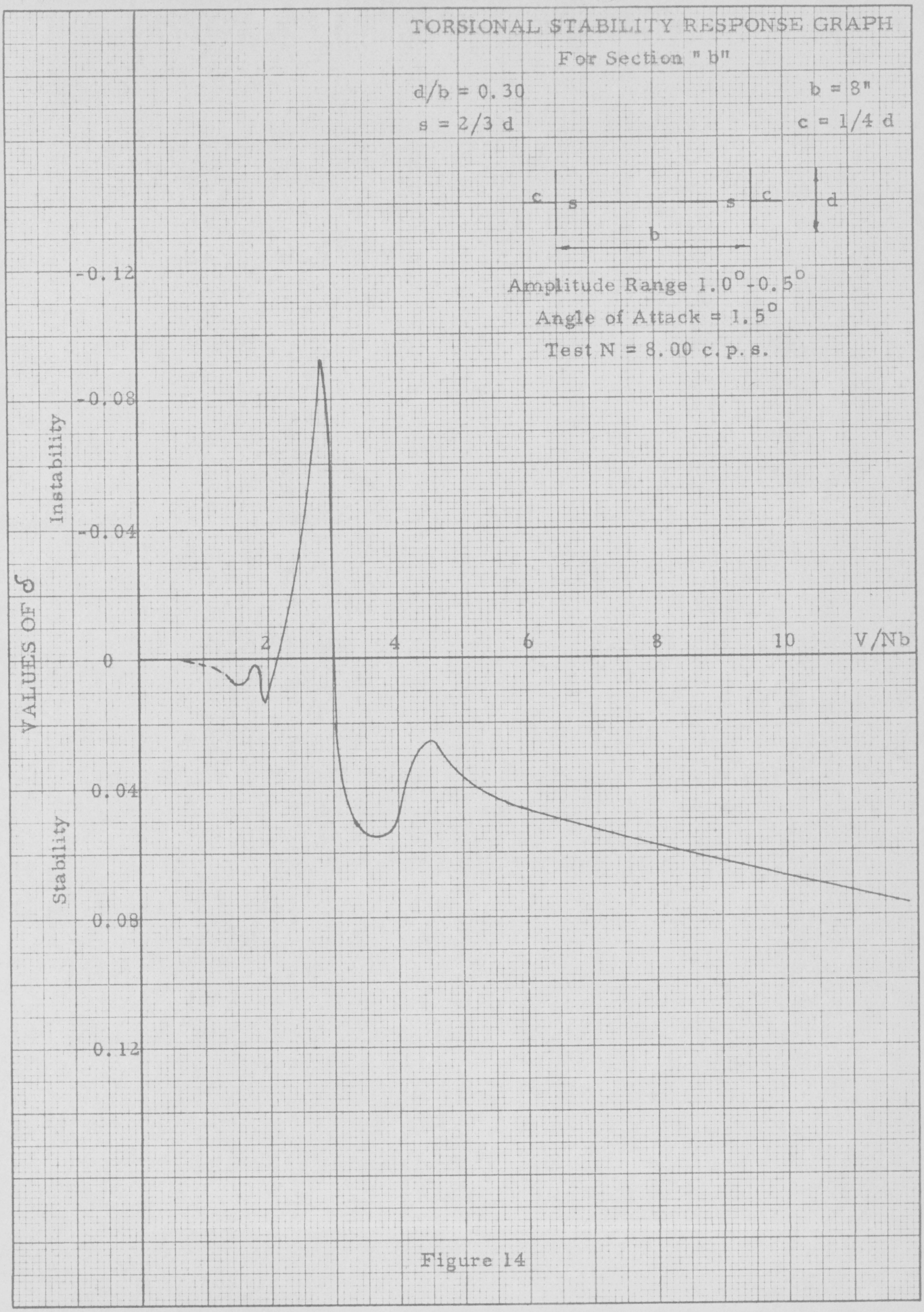
TORSIONAL STABILITY RESPONSE GRAPH
For Section " b"
d/b = 0.30
s = 2/3 d
b = 8"
c = 1/4 d
c
s
s
c
d
b
Amplitude Range 1.0°-0.5°
Angle of Attack = 1.5°
Test N = 8.00 c.p.s.
VALUES OF δ
Instability
Stability
-0.12
-0.08
-0.04
0
0.04
0.08
0.12
2
4
6
8
10
V/Nb

Figure 14

3. Section "c".

The static tests of section "c" (Figure 15) indicate slight vertical instability between values of -2° and +2°, angle of attack. Outside this range the section is vertically stable. The static moment graph indicates a stable region between -5.7° to +5.7°, angle of attack. Outside this range the section is torsionally unstable.

The dynamic tests for the vertical motion of section "c", Figure 16, indicate that above the velocity ratio of 2.2 the section is vertically stable. There is a range of slight limited instability between V/Nb of 1.5 to 2.2. Below velocity ratios of 2.2 the section is vertically stable. The section is torsionally unstable (Figure 17) above the critical velocity ratio of 10.6 and exhibits a high degree of limited instability between values of 1.9 and 3.2 (V/Nb). There are torsionally stable regions between velocity ratios of 0 to 1.9 and from 3.2 to 10.6.

4. Section "d".

Section "d" is similar to section "c" with a reduction in size of the center slot and the outside fins of section "d".

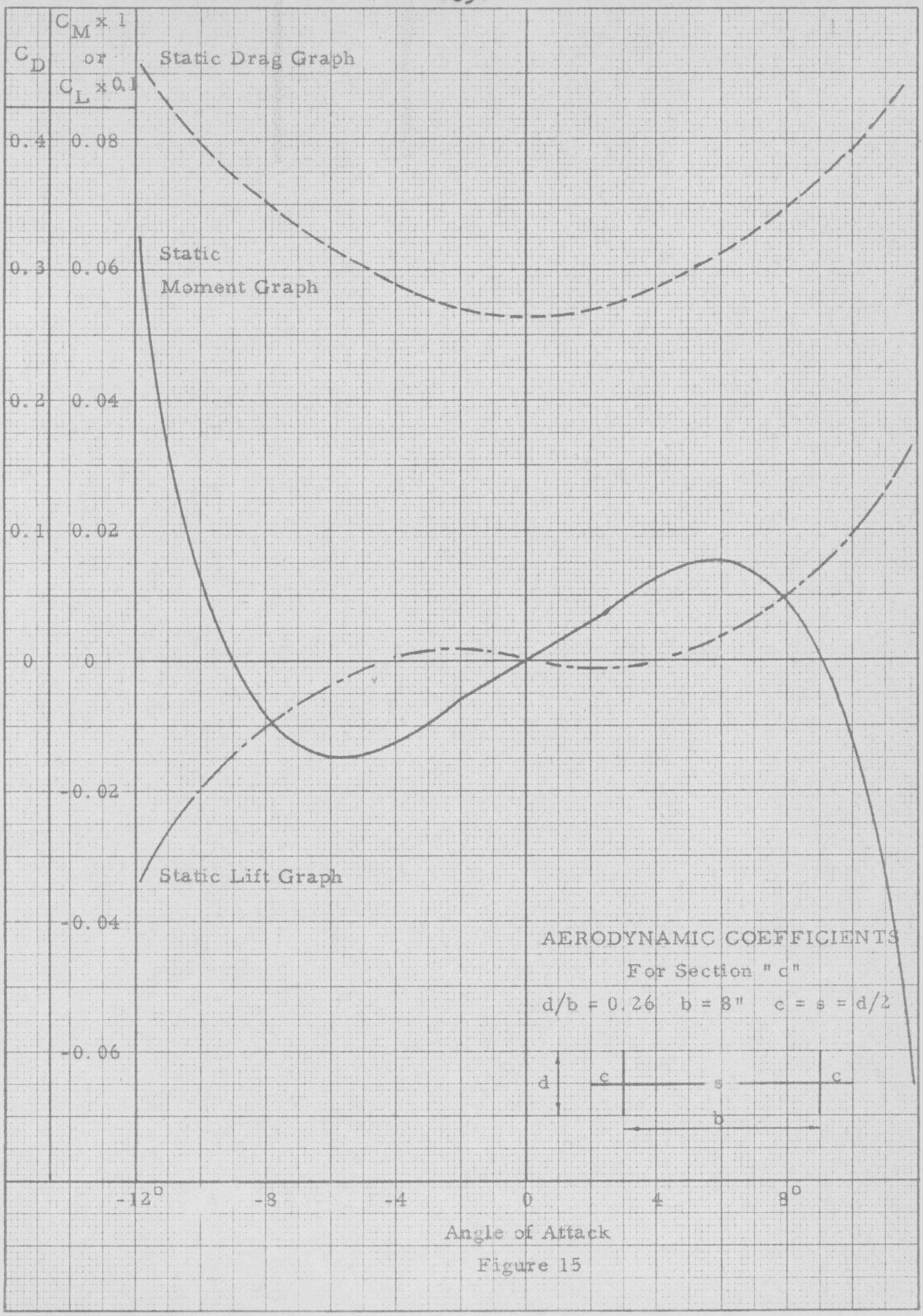
C_D
$C_M \times 1$ or $C_L \times 0.1$
Static Drag Graph
Static Moment Graph
Static Lift Graph
0.4
0.3
0.2
0.1
0
-0.02
-0.04
-0.06
0.08
0.06
0.04
0.02
0
-12°
-8
-4
0
4
8°
Angle of Attack
AERODYNAMIC COEFFICIENTS
For Section "c"
d/b = 0.26 b = 8" c = s = d/2
d
c
s
c
b

Figure 15

VERTICAL STABILITY RESPONSE GRAPH

For Section " c"

d/b = 0.26 b = 8" c = s = d/2

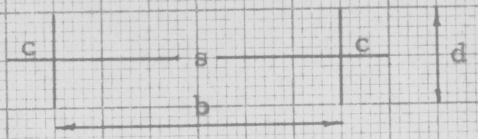

Amplitude Range 0.10" -0.05"

Angle of Attack = 1.5°

Test N = 9.58 c.p.s.

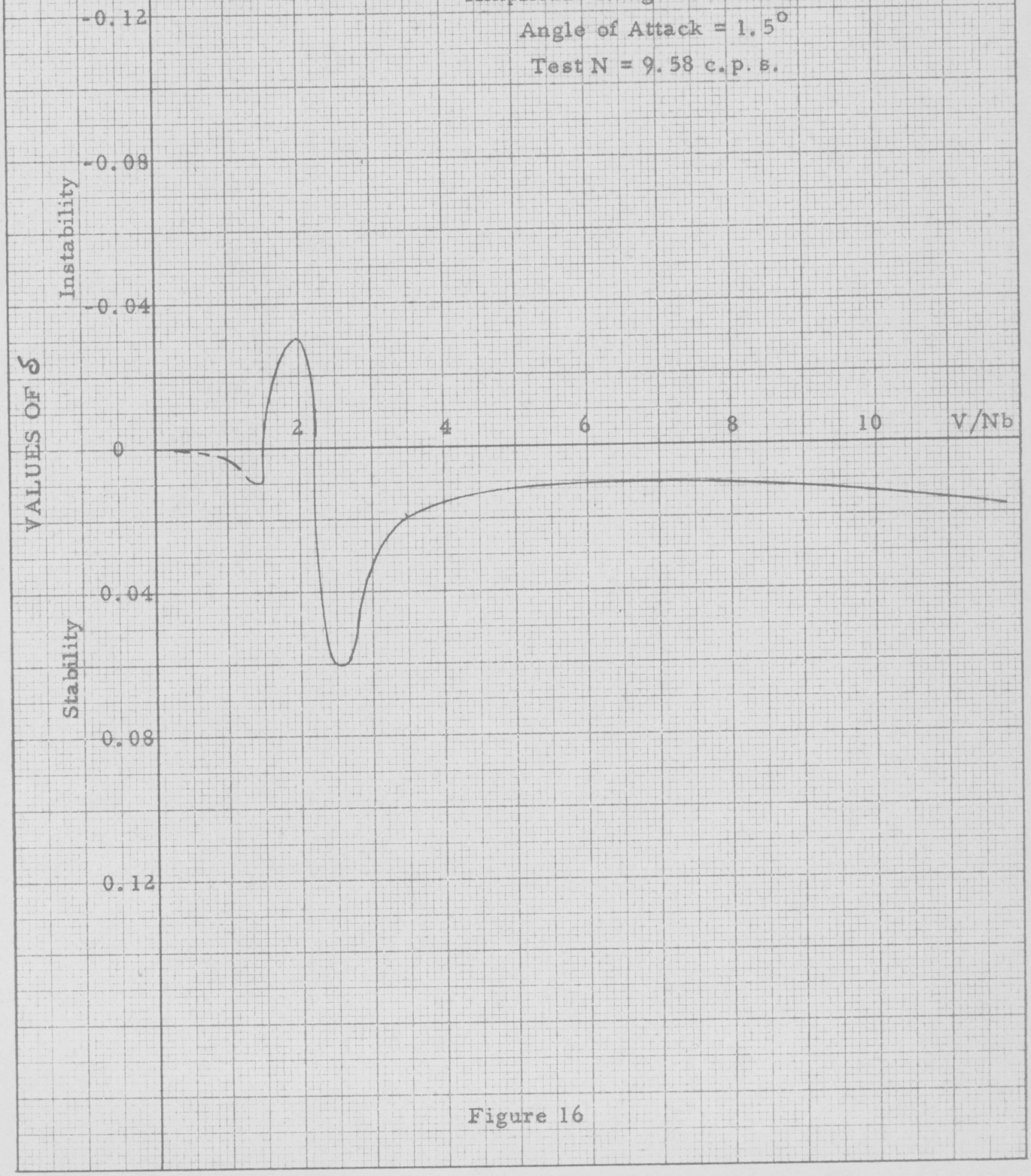

Figure 16

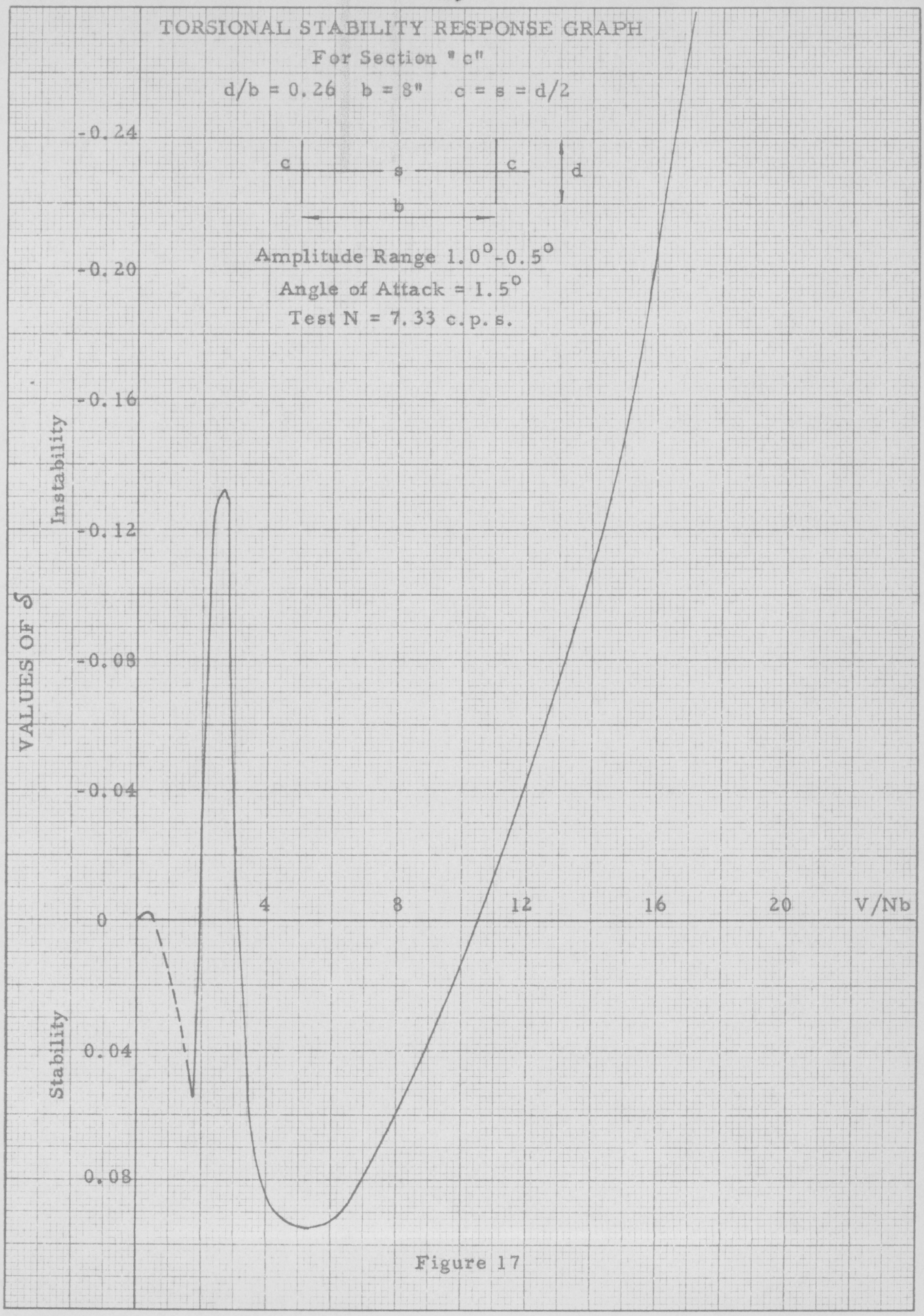
TORSIONAL STABILITY RESPONSE GRAPH
For Section "c"
d/b = 0.26 b = 8" c = s = d/2
c
s
c
d
b
Amplitude Range 1.0°-0.5°
Angle of Attack = 1.5°
Test N = 7.33 c.p.s.
VALUES OF δ
Instability
Stability
-0.24
-0.20
-0.16
-0.12
-0.08
-0.04
0
0.04
0.08
4
8
12
16
20
V/Nb

Figure 17

The static tests reveal (Figure 18) that section "d" is vertically unstable between angles of attack of -3° to +3°. Outside this range vertical stability is indicated. The section is torsionally unstable over the entire range of angle of attack.

The dynamic tests indicate that for vertical motion (Figure 19) the section is stable above velocity ratios of 2.1. There is a region of limited instability between velocity ratios of 1.6 and 2.1; whereas below 1.6 the section is vertically stable. Figure 20 reveals catastrophic torsional instability above the critical velocity ratio of 8.2. There is also a region of limited instability between V/Nb values of 2.0 and 3.4. Although there are two regions of stability for torsional motion, one between velocity ratios of 3.4 and 8.2, the other between 0 and 2.0, this section is highly undesirable because of its torsional catastrophic instability in the high ranges of V/Nb.

5. Section "e".

The static tests (Figure 21) indicate that the section is unstable over the entire range of angles of attack for vertical motion. Similarly, for torsional motion the section is basically unstable except for a

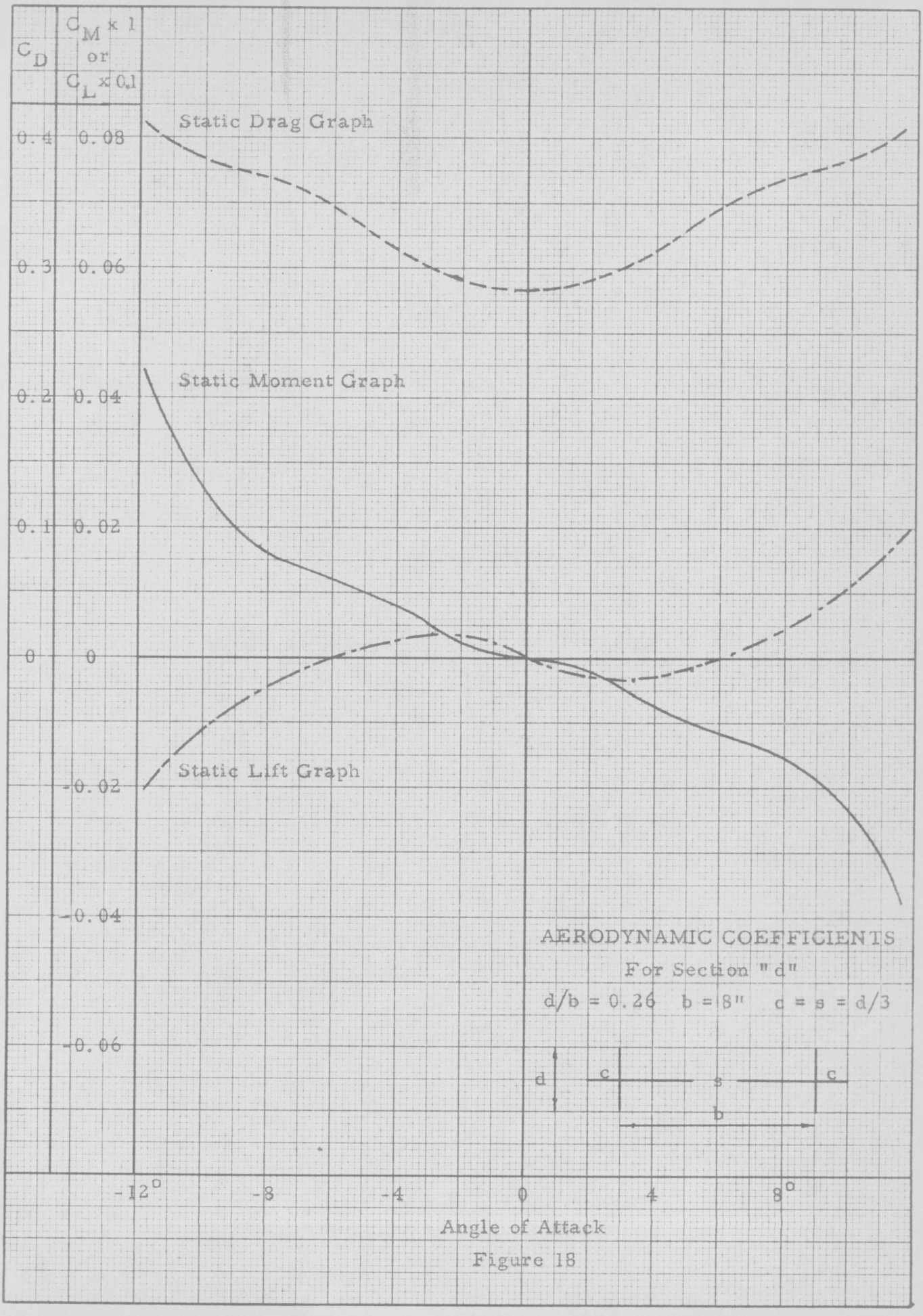
C_D
$C_M \times 1$ or $C_L \times 0.1$
Static Drag Graph
Static Moment Graph
Static Lift Graph
0.4
0.3
0.2
0.1
0
-0.02
-0.04
-0.06
0.08
0.06
0.04
0.02
0
-12°
-8
-4
0
4
8°
Angle of Attack
AERODYNAMIC COEFFICIENTS
For Section "d"
d/b = 0.26 b = 8" c = s = d/3
d
c
s
c
b

Figure 18

VERTICAL STABILITY RESPONSE GRAPH

For Section "d"

d/b = 0.26 b = 8" c = s = d/3

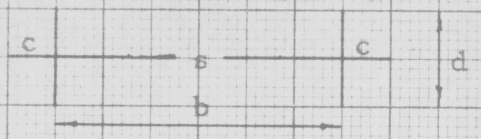

Amplitude Range 0.10" -0.05"

Angle of Attack = 1.5°

Test N = 9.62 c.p.s.

Figure 19

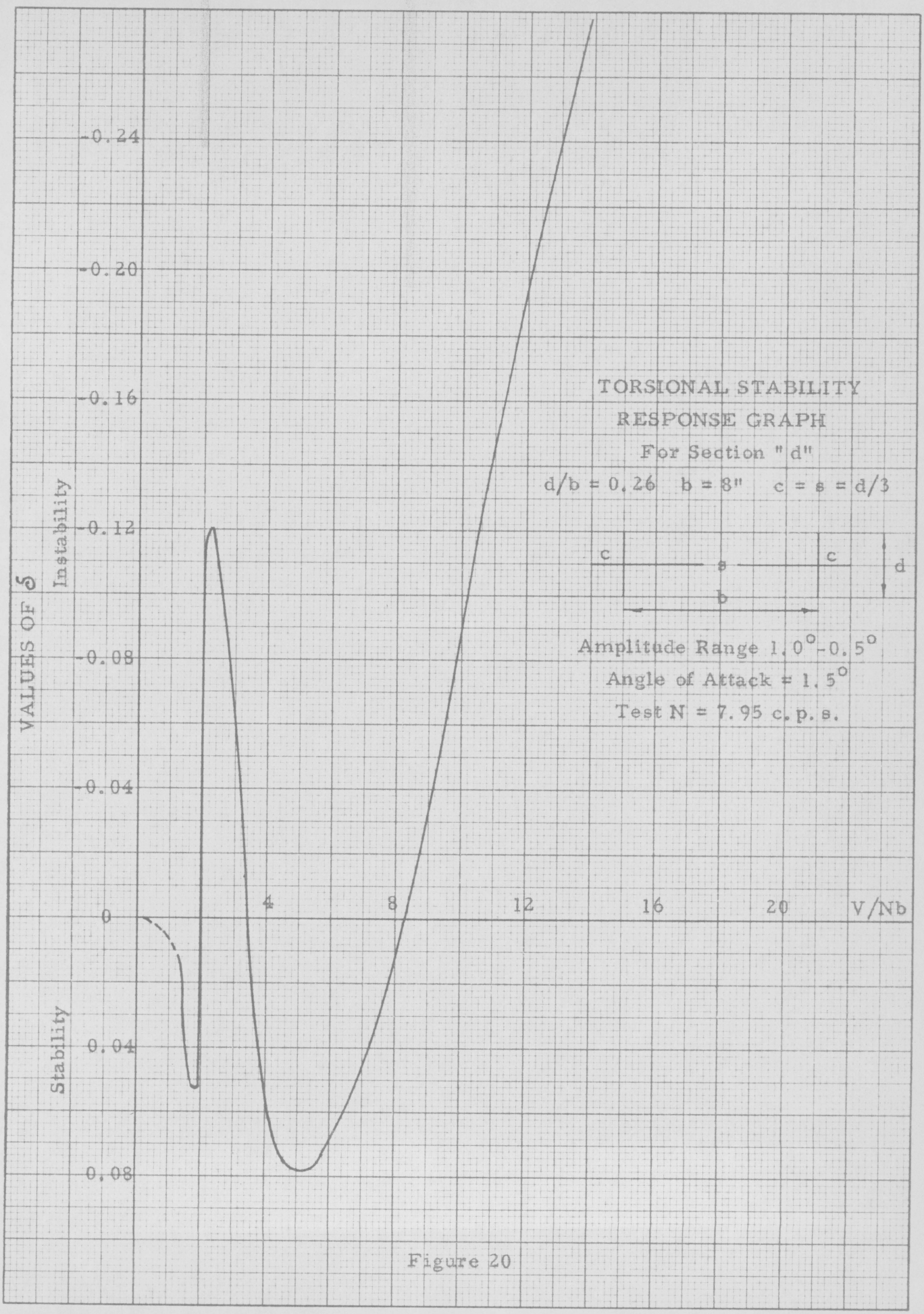
TORSIONAL STABILITY
RESPONSE GRAPH
For Section "d"
d/b = 0.26 b = 8" c = s = d/3
c
s
c
d
b
Amplitude Range 1.0°-0.5°
Angle of Attack = 1.5°
Test N = 7.95 c.p.s.
VALUES OF δ
Instability
Stability
-0.24
-0.20
-0.16
-0.12
-0.08
-0.04
0
0.04
0.08
4
8
12
16
20
V/Nb

Figure 20

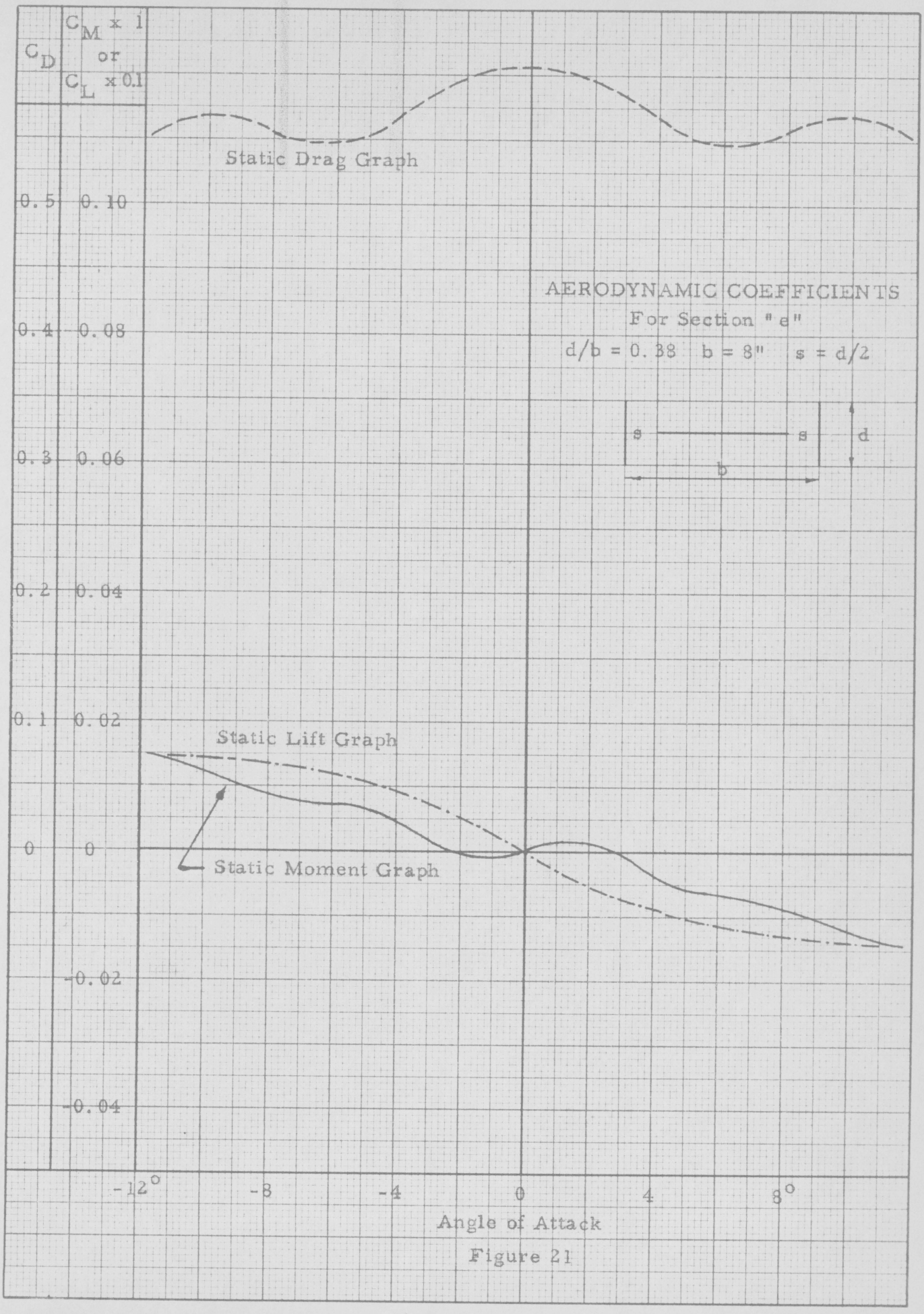
C_D
C_M x 1
or
C_L x 0.1
Static Drag Graph
AERODYNAMIC COEFFICIENTS
For Section "e"
d/b = 0.38 b = 8" s = d/2
s
s
d
b
0.5
0.4
0.3
0.2
0.1
0
0.10
0.08
0.06
0.04
0.02
0
-0.02
-0.04
Static Lift Graph
Static Moment Graph
-12°
-8
-4
0
4
8°
Angle of Attack

Figure 21

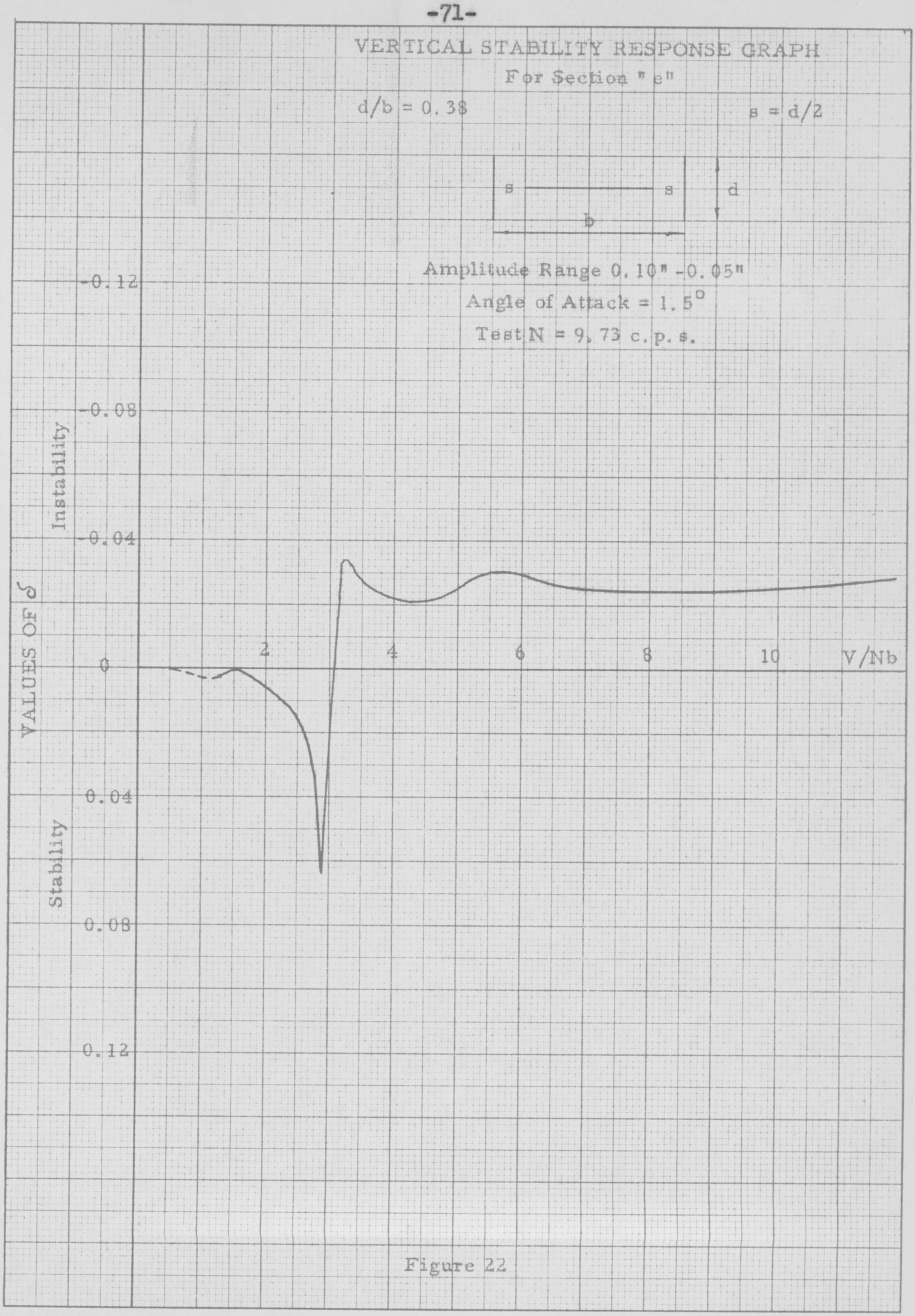
VERTICAL STABILITY RESPONSE GRAPH
For Section "e"
d/b = 0.38
s = d/2
s
s
d
b
Amplitude Range 0.10" -0.05"
Angle of Attack = 1.5°
Test N = 9.73 c.p.s.
VALUES OF δ
Instability
Stability
-0.12
-0.08
-0.04
0
0.04
0.08
0.12
2
4
6
8
10
V/Nb

Figure 22

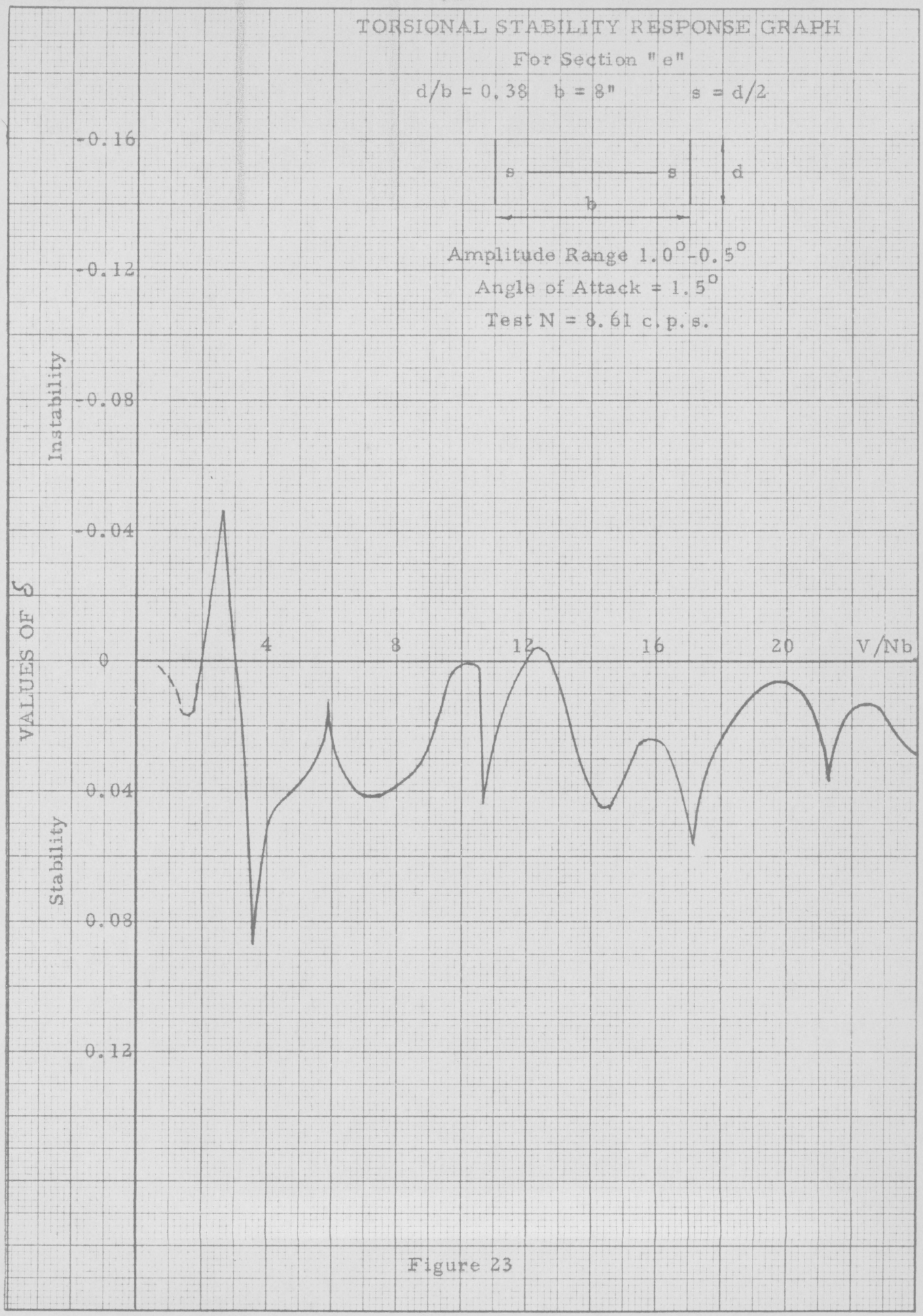
TORSIONAL STABILITY RESPONSE GRAPH
For Section "e"
d/b = 0.38 b = 8" s = d/2
s
s
d
b
Amplitude Range 1.0°-0.5°
Angle of Attack = 1.5°
Test N = 8.61 c.p.s.
-0.16
-0.12
-0.08
-0.04
0
0.04
0.08
0.12
Instability
Stability
VALUES OF δ
4
8
12
16
20
V/Nb

Figure 23

small region of stability between angles of attack of -1.2° to +1.2°.

The dynamic test for vertical motion (Figure 22) also shows an unstable condition above the critical velocity ratio of 3.1, although the decrement remains fairly constant and could be corrected if the structural damping were at least 0.03 in the structure. For torsional motion a rather erratic curve was obtained, as can be seen in Figure 23. For velocity ratios above 3.1 the section is torsionally stable except for a very limited instability condition between V/Nb of 12.0 and 12.7 which is not serious at all. There is another region of non-catastrophic torsional instability between V/Nb of 2.0 and 3.1, however, this too is not serious.

6. Girder H-Section.

Figures 24 through 27 indicate the effect of initial test amplitude on the magnitude of the peak decrements in regions of both stability and limited instability for vertical motion. The initial test amplitude is the initial displacement given the section before it is allowed to oscillate freely in the air stream. It is seen that the general shape of the stability response graph is preserved in these four tests but the magnitude of the

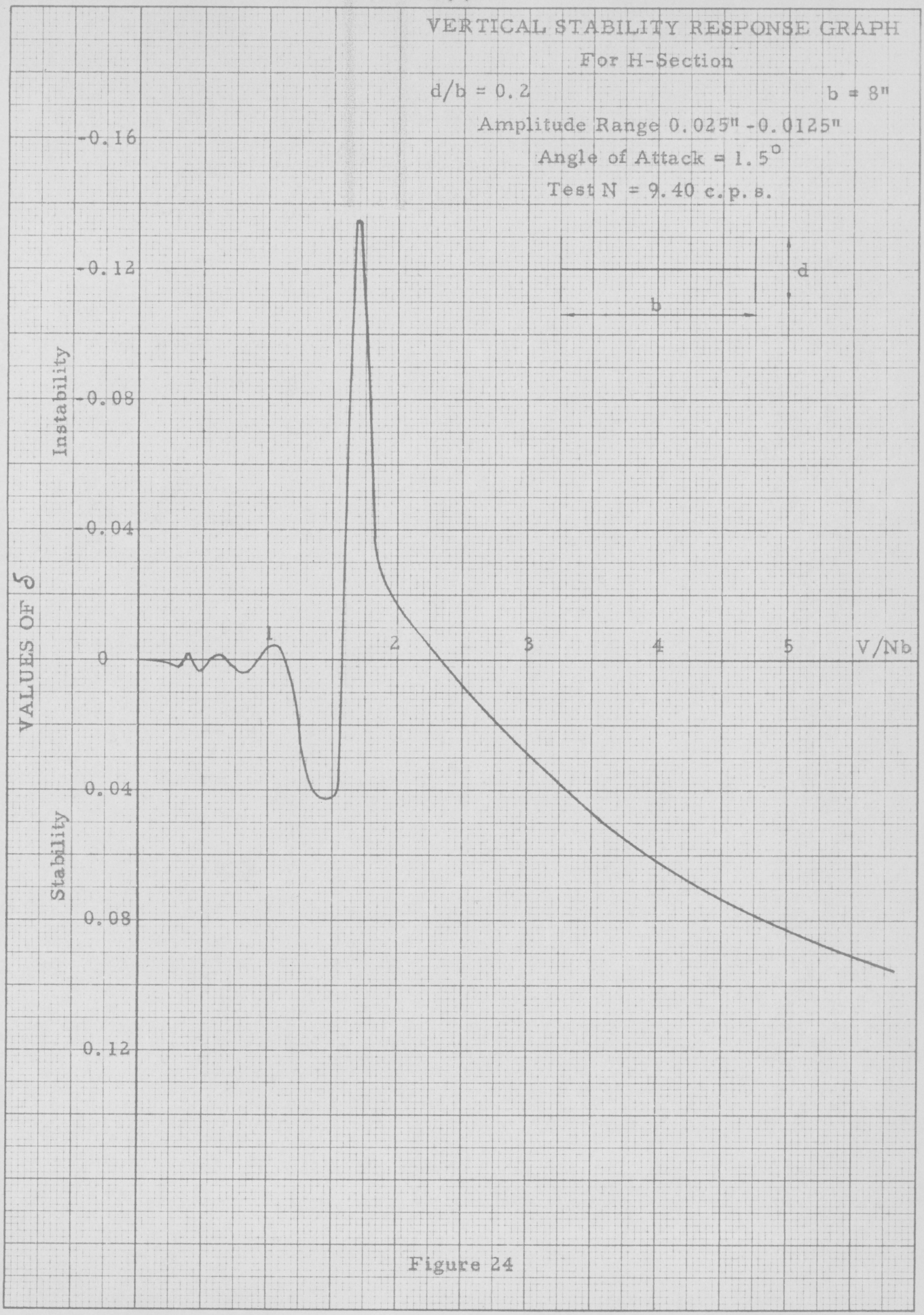
VERTICAL STABILITY RESPONSE GRAPH
For H-Section
d/b = 0.2
b = 8"
Amplitude Range 0.025" -0.0125"
Angle of Attack = 1.5°
Test N = 9.40 c.p.s.
d
b
VALUES OF δ
Instability
Stability
-0.16
-0.12
-0.08
-0.04
0
0.04
0.08
0.12
1
2
3
4
5
V/Nb

Figure 24

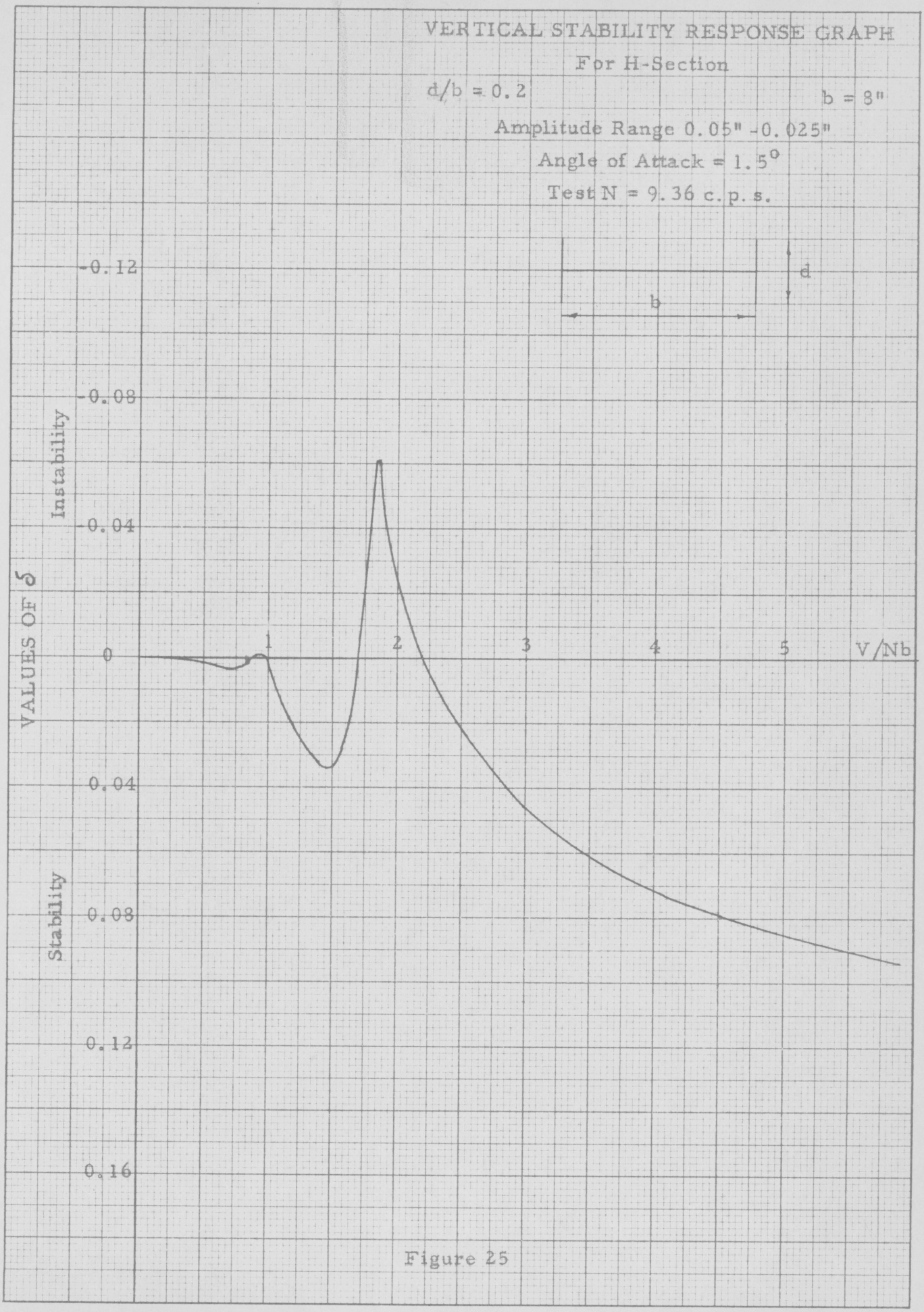
VERTICAL STABILITY RESPONSE GRAPH
For H-Section
d/b = 0.2
b = 8"
Amplitude Range 0.05" -0.025"
Angle of Attack = 1.5°
Test N = 9.36 c.p.s.
d
b
VALUES OF δ
Instability
Stability
-0.12
-0.08
-0.04
0
0.04
0.08
0.12
0.16
1
2
3
4
5
V/Nb

Figure 25

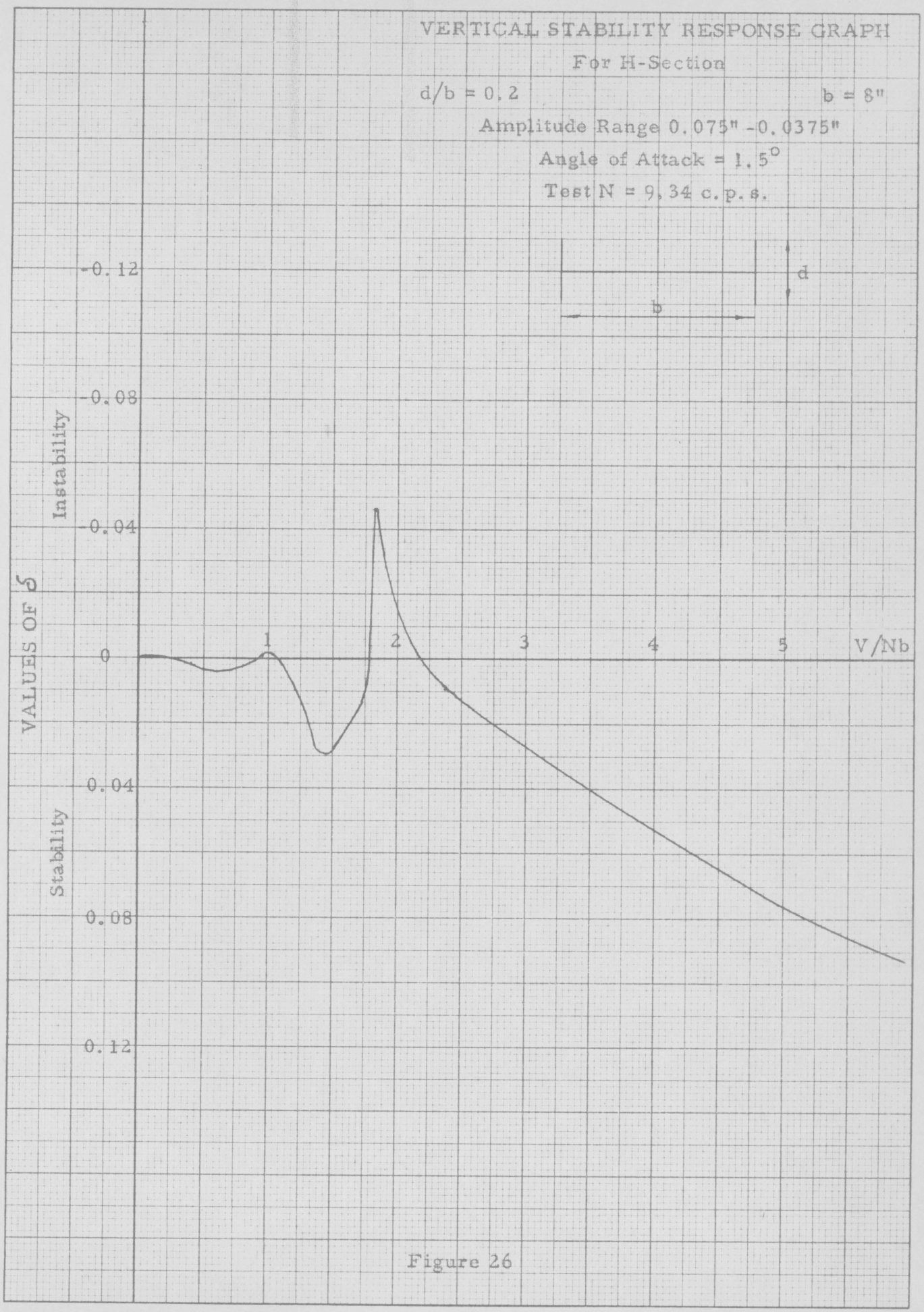
VERTICAL STABILITY RESPONSE GRAPH
For H-Section
d/b = 0.2
b = 8"
Amplitude Range 0.075" -0.0375"
Angle of Attack = 1.5°
Test N = 9.34 c.p.s.
d
b
VALUES OF δ
Instability
Stability
-0.12
-0.08
-0.04
0
0.04
0.08
0.12
1
2
3
4
5
V/Nb

Figure 26

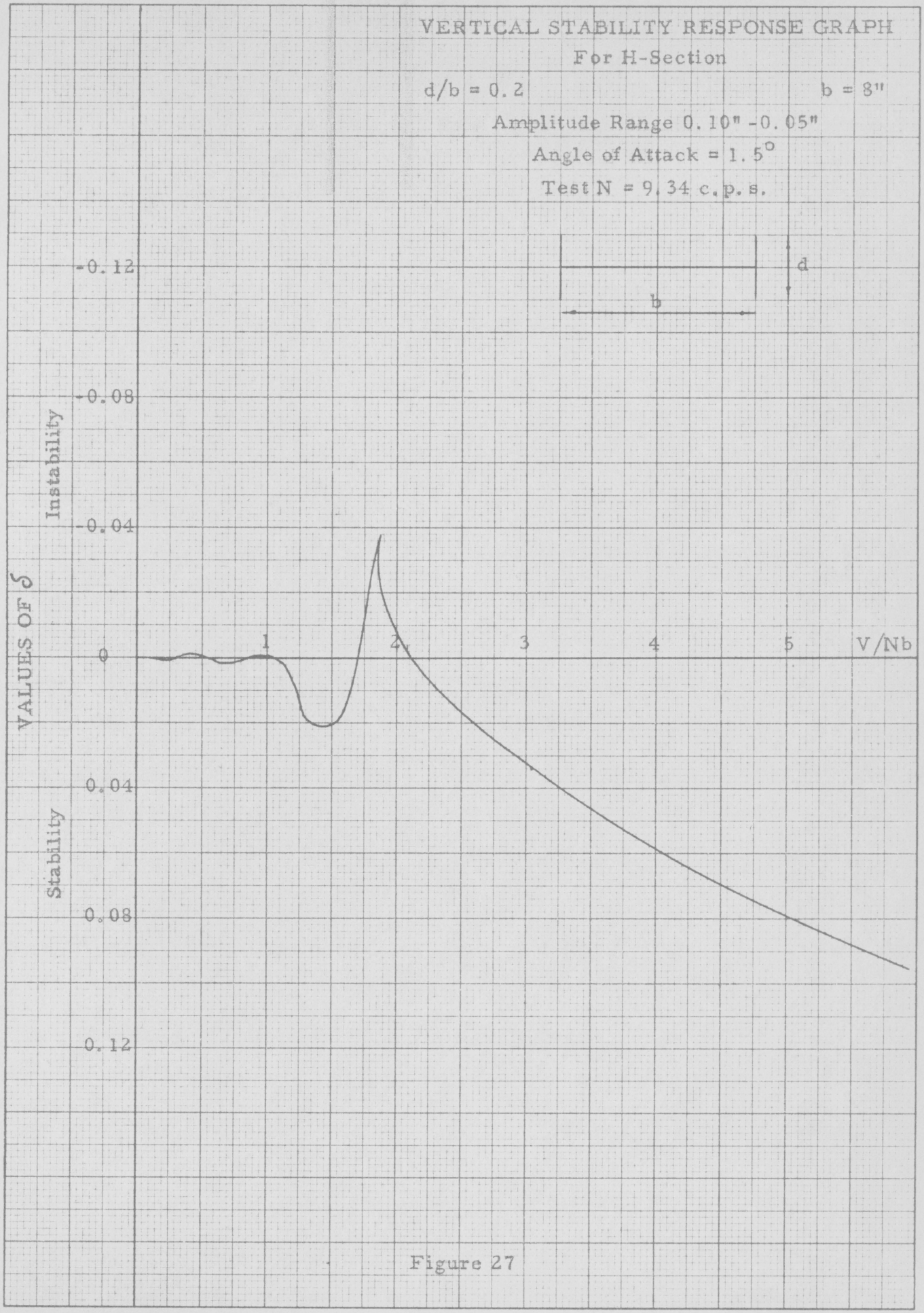
VERTICAL STABILITY RESPONSE GRAPH
For H-Section
d/b = 0.2
b = 8"
Amplitude Range 0.10" -0.05"
Angle of Attack = 1.5°
Test N = 9.34 c.p.s.
d
b
VALUES OF δ
Instability
Stability
-0.12
-0.08
-0.04
0
0.04
0.08
0.12
1
2
3
4
5
V/Nb

Figure 27

peak decrements in each region decreases as the initial test amplitude is increased. A similar conclusion is reached from the torsional motion dynamic tests in Figures 28 through 31.

Figure 32 represents a summary of the information regarding amplitude effect on logarithmic decrement obtained from Figures 24 through 31. The curves obtained for vertical motion from actual tests are shown in Figure 32 as solid lines between the amplitude ranges of 0.025 to 0.10 inch. Outside this range these curves are shown dashed to indicate their probable paths. The graph (Figure 32) for vertical motion in the unstable region represents the maximum decrements for the last region of limited instability in Figures 24 through 27. The graph (Figure 32) for vertical motion in the stable region represents the maximum decrements of the stable region preceding the region of maximum non-catastrophic instability in Figures 24 through 27. The curves obtained for torsional motion from actual tests are shown in Figure 32 as alternate dots and dashes between the amplitude ranges of 0.25 to 1.0 degree. Outside this range these curves are shown dashed to indicate their probable paths. The graph in Figure 32 for torsional motion in the stable region

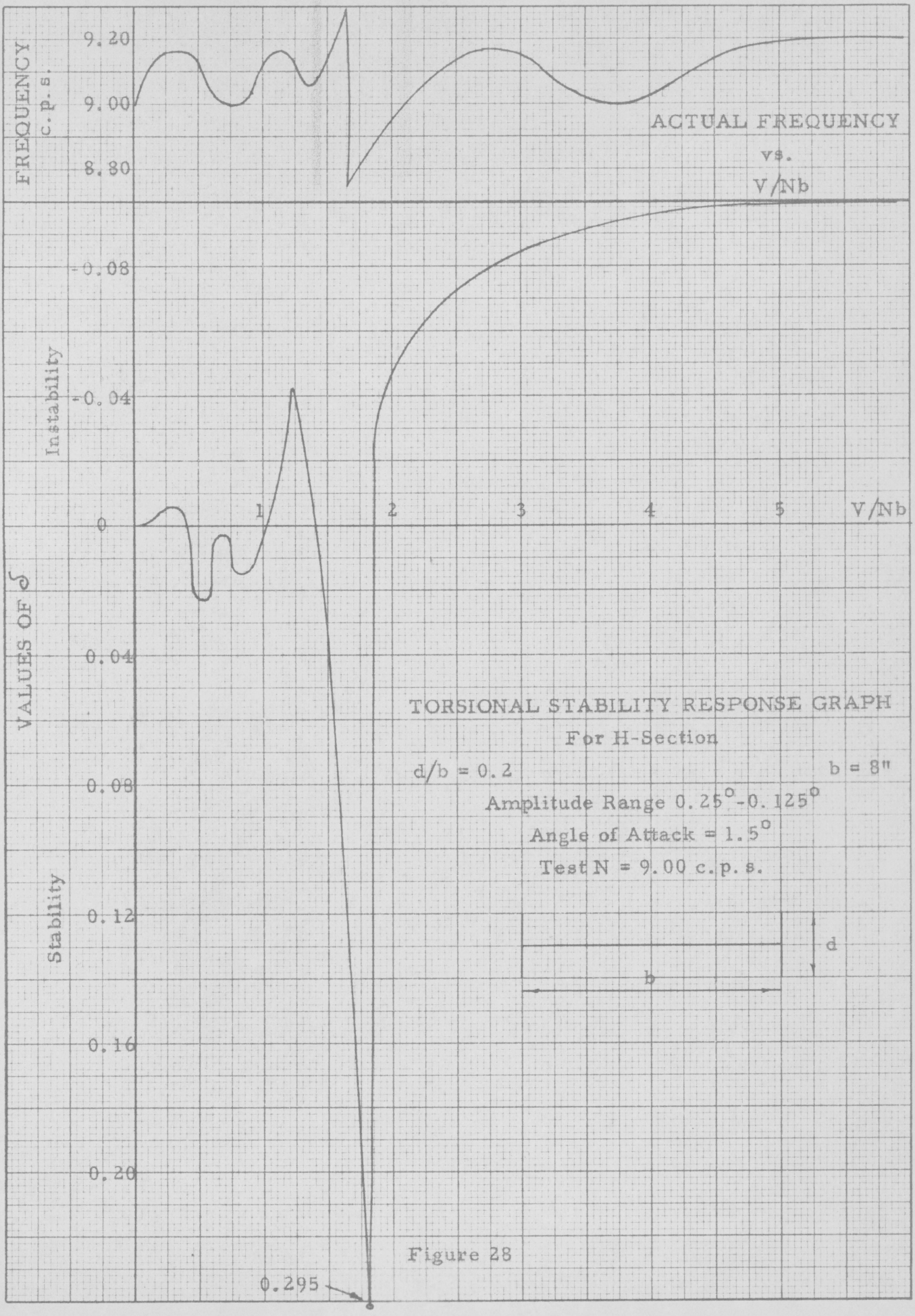
FREQUENCY c.p.s.
9.20
9.00
8.80
ACTUAL FREQUENCY
vs.
V/Nb
VALUES OF δ
Instability
Stability
0.08
0.04
0
0.04
0.08
0.12
0.16
0.20
1
2
3
4
5
V/Nb
0.295
TORSIONAL STABILITY RESPONSE GRAPH
For H-Section
d/b = 0.2
b = 8"
Amplitude Range 0.25°-0.125°
Angle of Attack = 1.5°
Test N = 9.00 c.p.s.
d
b

Figure 28

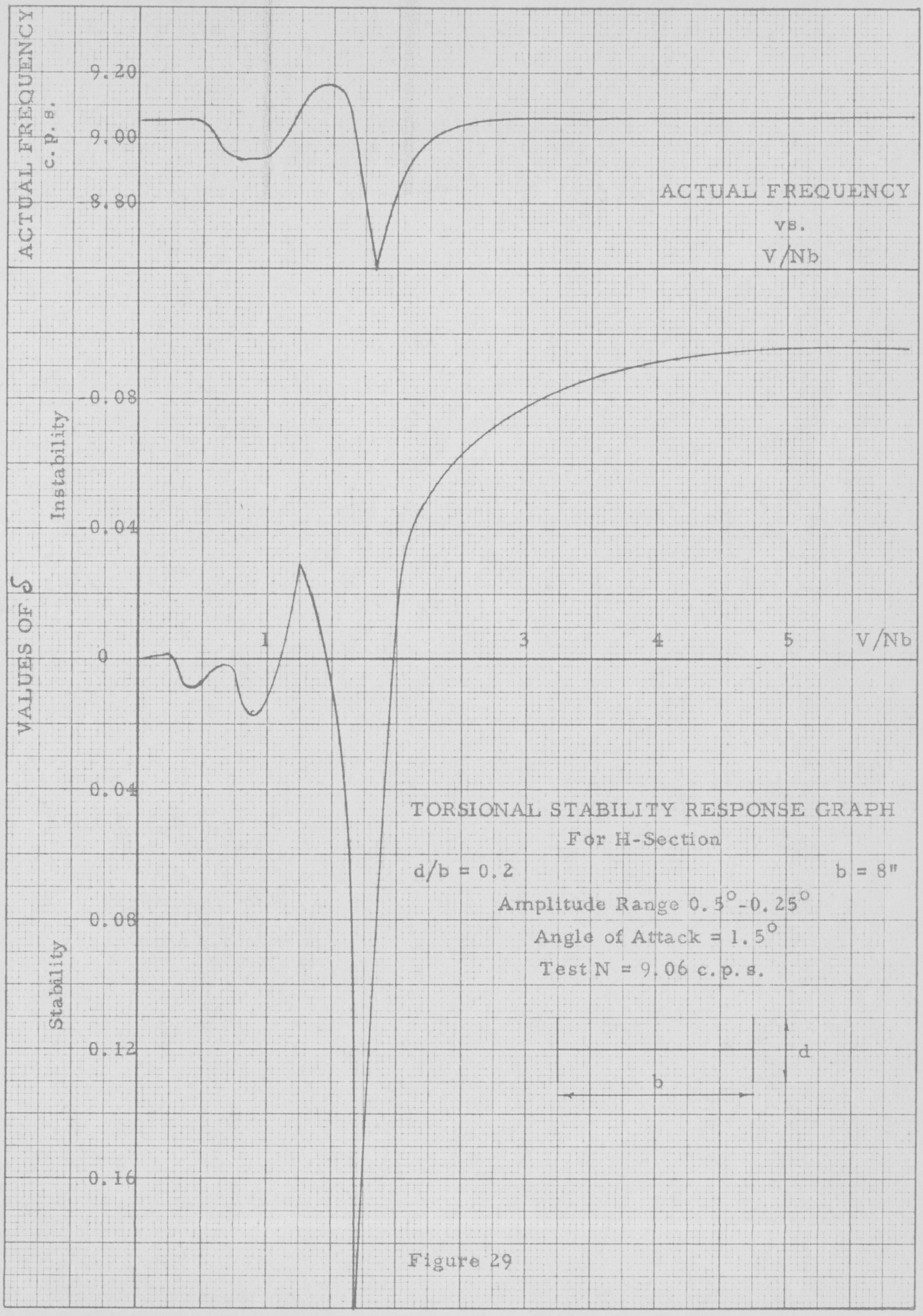
ACTUAL FREQUENCY
c.p.s.
9.20
9.00
8.80
ACTUAL FREQUENCY
vs.
V/Nb
VALUES OF δ
Instability
-0.08
-0.04
0
1
3
4
5
V/Nb
0.04
0.08
Stability
0.12
0.16
TORSIONAL STABILITY RESPONSE GRAPH
For H-Section
d/b = 0.2
b = 8"
Amplitude Range 0.5°-0.25°
Angle of Attack = 1.5°
Test N = 9.06 c.p.s.
d
b

Figure 29

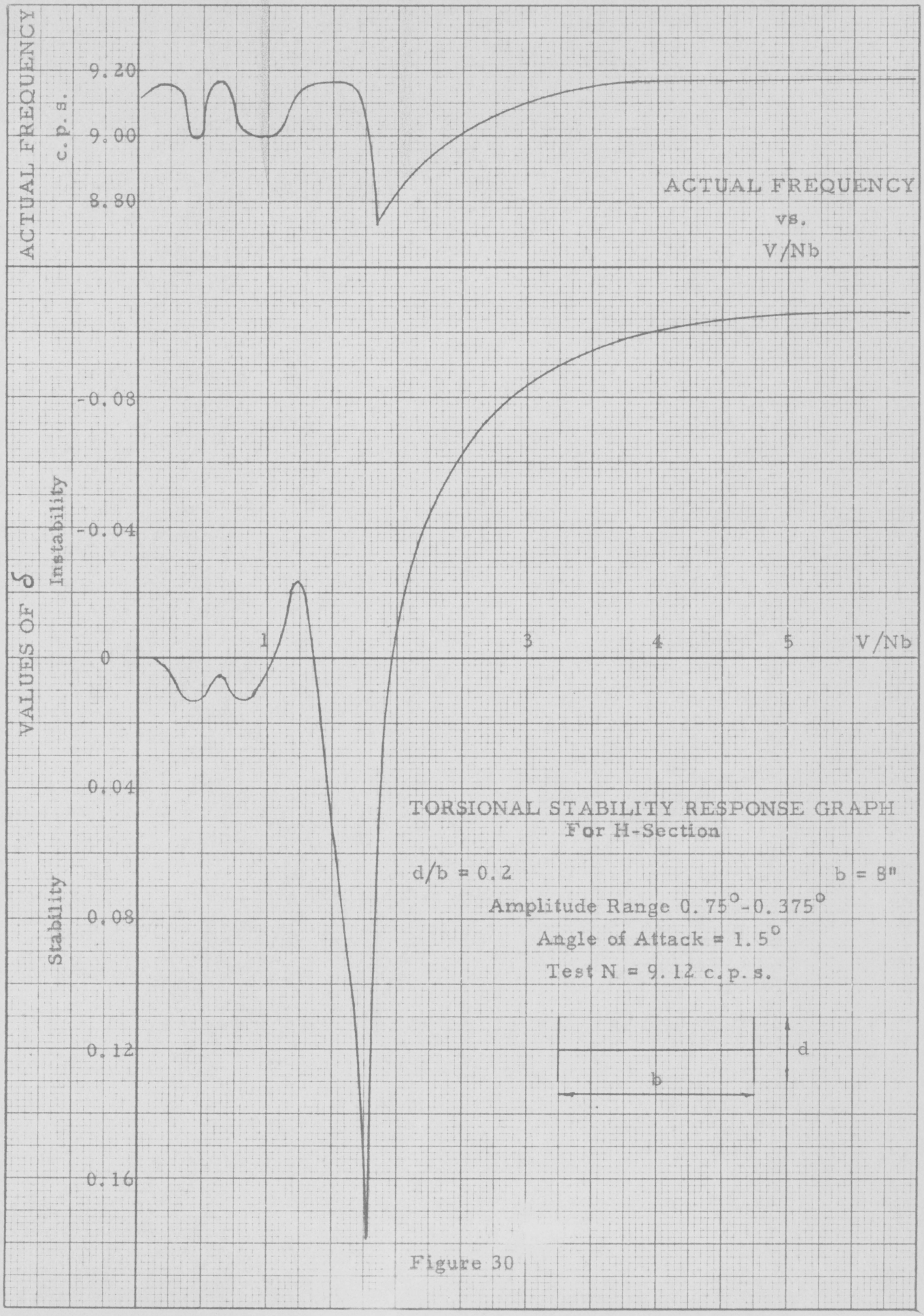
ACTUAL FREQUENCY
c.p.s.
9.20
9.00
8.80
ACTUAL FREQUENCY
vs.
V/Nb
VALUES OF δ
Instability
Stability
-0.08
-0.04
0
0.04
0.08
0.12
0.16
1
3
4
5
V/Nb
TORSIONAL STABILITY RESPONSE GRAPH
For H-Section
d/b = 0.2
b = 8"
Amplitude Range 0.75°-0.375°
Angle of Attack = 1.5°
Test N = 9.12 c.p.s.
d
b

Figure 30

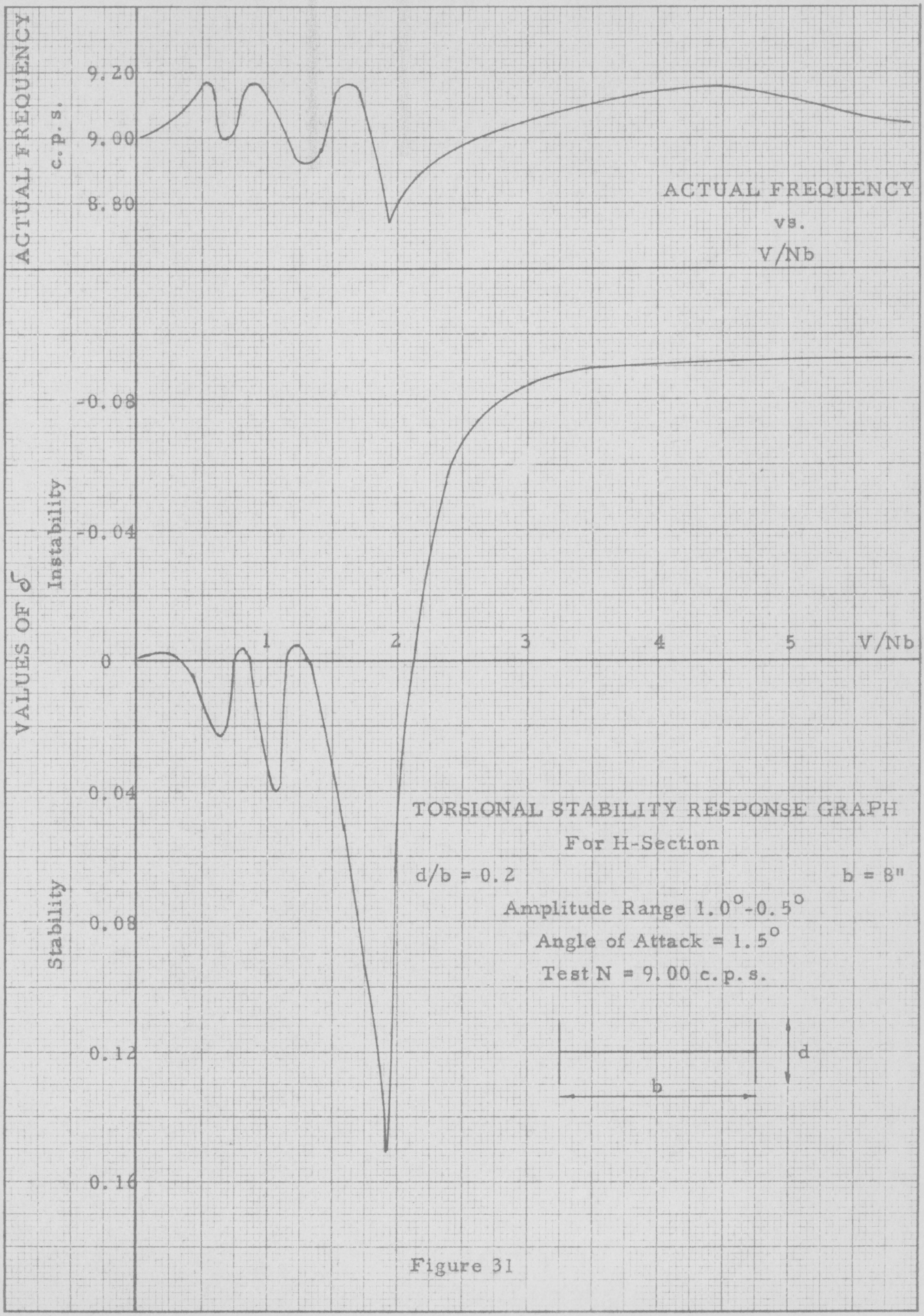
ACTUAL FREQUENCY
c.p.s.
9.20
9.00
8.80
ACTUAL FREQUENCY
vs.
V/Nb
VALUES OF δ
Instability
-0.08
-0.04
0
1
2
3
4
5
V/Nb
0.04
Stability
0.08
0.12
0.16
TORSIONAL STABILITY RESPONSE GRAPH
For H-Section
d/b = 0.2
b = 8"
Amplitude Range 1.0°-0.5°
Angle of Attack = 1.5°
Test N = 9.00 c.p.s.
d
b

Figure 31

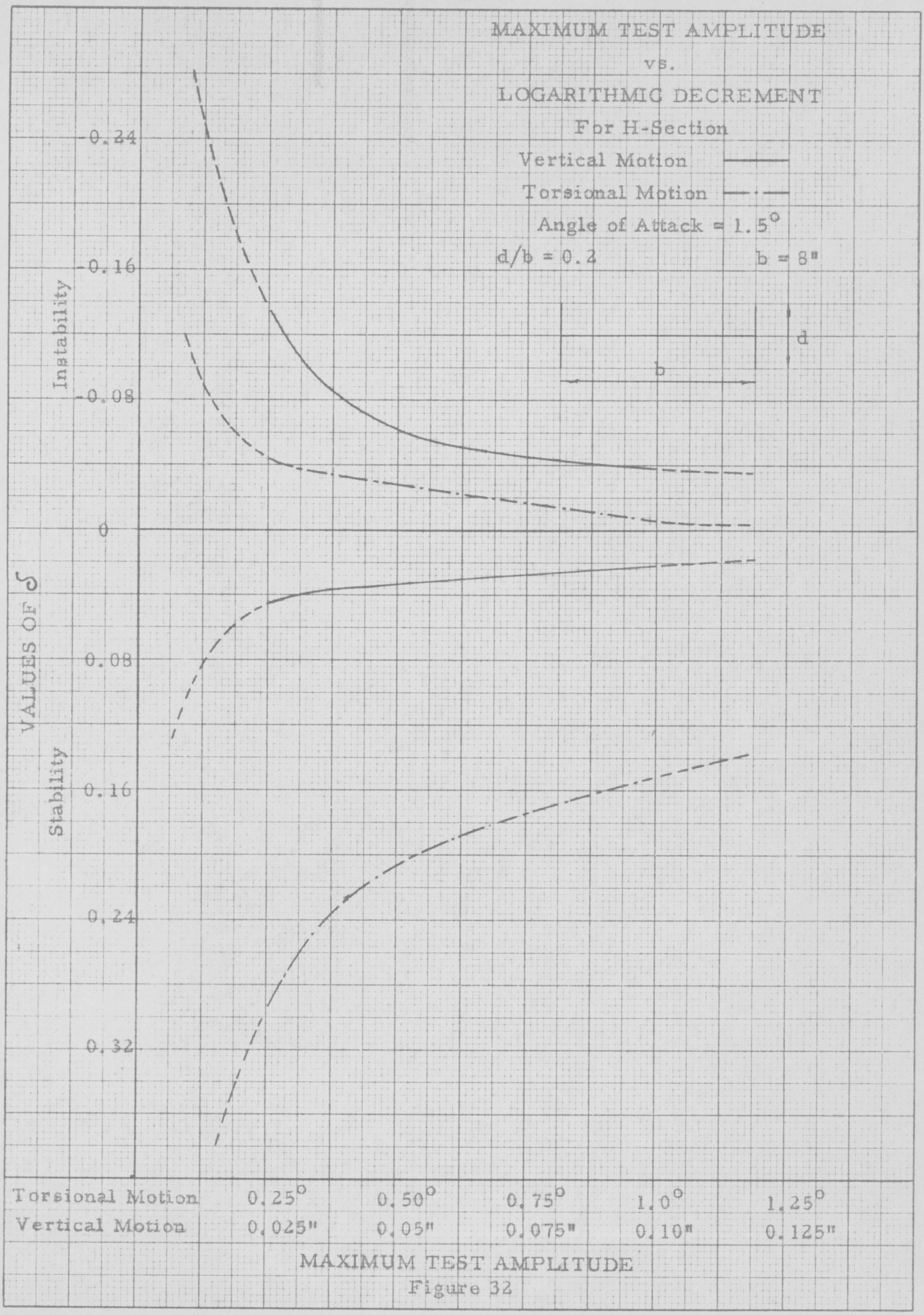
MAXIMUM TEST AMPLITUDE
vs.
LOGARITHMIC DECREMENT
For H-Section
Vertical Motion
Torsional Motion
Angle of Attack = 1.5°
d/b = 0.2
b = 8"
d
b
VALUES OF δ
Instability
Stability
-0.24
-0.16
-0.08
0
0.08
0.16
0.24
0.32
Torsional Motion 0.25° 0.50° 0.75° 1.0° 1.25°
Vertical Motion 0.025" 0.05" 0.075" 0.10" 0.125"
MAXIMUM TEST AMPLITUDE

Figure 32

represents the maximum decrements obtained from the last stable regions in Figures 29 through 31. The graph in Figure 32 for torsional motion in the unstable region represents the maximum decrements of the region preceding the region of maximum torsional stability in Figures 29 through 31.

Another interesting phenomenon observed in the torsional motion tests was the variation in frequency at various velocity ratios. The H-section considered was catastrophically unstable in torsion above critical velocity ratios ranging from 1.85 to 2.15. In every case the actual frequency in the last stable region (just below the critical velocity ratio) was considerably less than the natural frequency. The same phenomenon was noted for the stable region preceding the range of greatest limited instability for the vertical motion tests, although this frequency variation was not plotted.

VI. DISCUSSION OF RESULTS

A. TEST RESULTS

The thesis that static tests on section models reveal the basic stability characteristics of these sections was confirmed in these tests with two exceptions, both of which have possible explanations.

1. Section "a".

This section is acceptable from the standpoint of aerodynamic stability. The dynamic tests substantiate the static tests in that both indicate basically a neutral section for angles of attack in the vicinity of 1.5°. Although the dynamic test for vertical motion indicates a section which is slightly unstable between V/Nb of 5.0 and 11.0, this negative decrement is so small (maximum of -0.01) that it most likely would be corrected by structural damping. In the dynamic test for torsional motion it can be seen that although the region of rather high non-catastrophic instability might cause some difficulty, the section is basically stable.

2. Section "b".

This section is not as acceptable as section "a" because of the higher degree of vertical instability

above V/Nb of 3.0. Again there is good agreement between the static and dynamic tests. The changes in the proportions of girder depth and slot width in section "b" have improved the torsional properties of the section while increasing the vertical instability as compared to section "a". However, since the vertical stability response graph seems to indicate a neutral section with the reference axis shifted down somewhat, a fair amount of structural damping in the neighborhood of 0.04 would most likely render this an acceptable section. Throughout the testing a pronounced beat effect was noted at various times on the time-displacement record, indicating the action of more than one variable force at different frequencies. This effect was very pronounced above velocity ratios of 3.0 for the vertical motion dynamic test of this section.

3. Section "c".

This section is not aerodynamically stable because of an indicated catastrophic torsional instability above velocity ratios of 10.6. For this case the static moment graph indicated torsional stability for a range of angles of attack between -5.7° to +5.7° which did not agree with the torsional motion dynamic test as can be seen. It may be, however, that above velocity ratios of 18.7 the

section does become torsionally stable, since this was the highest run made on this section. However, it appeared impracticable to go higher because of the structural strength of the model and of the system itself. Since the negative damping at a V/Nb of 18.7 was -0.378 (not shown on graph, Figure 17) it is highly improbable that the structure could survive this range even if there were a stable region at a higher velocity ratio. It must be kept in mind, however, that this section is torsionally unstable above a velocity ratio of 10.6 which is very high for this type of test. For the actual structure, if a V/Nb of 10.6 meant a wind velocity greater than expected, this might be considered an acceptable section. The only difficulty would then be the torsionally non-catastrophic unstable range present, which, however, would be reduced by structural damping. As has been stated previously, some actual bridges have been found to have structural damping in the neighborhood of 0.05 to 0.10[7].

4. Section "d".

This section, like section "c", is not aerodynamically stable because of an indicated catastrophic torsional instability above velocity ratios of 8.2. For this case the static moment graph indicates this torsionally unstable condition. The static lift graph also

indicates vertical instability between angles of attack of -3° and +3°. Although the vertical stability response graph for this section shows a stable condition from V/Nb of 2.1 to at least 12.0, it does appear that it might cross the axis at a higher value of V/Nb, which would then substantiate the static lift graph. This section would be in the same category as section "c", i.e., if a V/Nb of 8.2 for section "d" corresponds to an excessive wind velocity for the prototype, then this too would be an acceptable section.

5. Section "e".

This section is not aerodynamically stable because of an indicated vertically unstable range above velocity ratios of 3.1. However, since the decrement in the range above V/Nb of 3.1 seems to be fairly constant, if the actual structure were capable of damping to the extent of approximately 0.035, the section could be considered acceptable. For this section the static tests again predict the behavior found from the dynamic tests. The erratic behavior of this section in the higher ranges of V/Nb, although practically entirely within the stable region, is quite different from the usual graphs obtained.

6. Girder H-Section.

The dynamic tests on the girder H-section at varying initial amplitudes partially confirm the theory proposed by Dr. Steinman[20,21] concerning the forced motion or vortex effect on suspension bridge sections. From the equation developed on page 35 where

$$\delta_n = \delta_a - \delta_s = \delta_s \cdot \frac{\omega}{\omega_n}\left(\frac{a_o - a}{a}\right)$$

it is evident that the following is true:

$a = a_o$	then	$\delta_a = \delta_s$
$a = o$	then	$\delta_a = \infty$
$a > a_o$	then	$\delta_a - \delta_s < 0$

This expression was developed for an arbitrary external harmonic force acting on a body. By examining a summary of the results of the dynamic tests on the girder H-section in Figure 32, it is seen that the curves presented could represent solutions for the aerodynamic damping in the above expression. The curves certainly seem to satisfy the three conditions which are evident from the expression, i.e.,

1. At the steady state amplitude the structural damping is equivalent to the aerodynamic damping.

2. As the initial amplitude approaches zero the aerodynamic damping increases and could presumably approach infinity.

3. When the initial amplitude is greater than the steady state amplitude, the net damping (the difference between aerodynamic and structural damping) is negative which in this case indicates a stable condition.

Since the curves (Figure 32) seem to satisfy this forced motion expression, it is reasonable to conclude that some forced vibration as well as self-excited vibration is taking place in the oscillations of the section during the tests. The fact that the frequency of vibration does not remain constant during a test run also seems to indicate the influence of a forced vibration effect in certain ranges which affects or controls the frequency of the oscillations. This vortex effect would explain the discrepancies existing between the present theory[19] (based on self-excited oscillations) and the experimental results; especially the difference between the existence of sharp peak decrements (in both stable and limited unstable regions) found by experiment and the smoother curve developed from theory. This difference would then be attributed to resonance effects causing

sharp peaks (representing forced vibrations) superimposed upon the basic curves obtained from the general theory[19] (due to self-excited vibrations)[13]. The magnitude of the contribution of the forced motion effect to the peak decrement values is a variable one, depending at least upon the initial amplitude, as was evident from the dynamic tests of the girder H-section. Since a forced motion has a limiting amplitude, these resonance effects occur only in stable regions and regions of limited instability. In regions of catastrophic instability, the forced motion effect may contribute to some extent towards initiating the oscillations which ultimately result in the destruction of the structure, however, in this region the self-excited vibrations are the primary cause of failure since they have no limiting amplitude.

Another indication of the presence of a forced motion was the beat effect noticed at various times during the tests, which implies the existence of more than one forcing function (self-excited motion and forced motion) acting at different frequencies.

An important question arises concerning the range over which <u>periodic</u> vortex shedding occurs. There is some uncertainty regarding the influence of Reynolds'

Number (R) on the frequency of vortex discharge for section models and for their prototypes. Since the R at which wind tunnel tests on section models are run differs considerably from the R which exists for prototypes at comparable V/Nb values, the danger exists of applying results for one type of flow condition in the model to an entirely different condition in the prototype. As an example of the difference in range of R between model and prototype: for a V/Nb of 1.7 and air at standard conditions, the R for the vertical motion tests of the girder H-section (d/b = 0.2) was approximately 9,200, whereas for a prototype the size of the Tacoma Bridge the R would be approximately 436,000. Although the variation of vortex frequency with respect to Reynolds' Number for this type of section is not known, there is much information concerning vortex effects on circular cylinders which might serve as a guide concerning what to expect on a bridge section. A circular cylinder exhibits periodic vortex discharges, where the frequency is a linear function of the velocity, over the entire range of Reynolds' Numbers from 1,000 to 500,000[22]. Beyond this range there is some question as to whether or not <u>periodic</u> vortex shedding takes place. "However, in connection with a

recent investigation, Krzywoblocki has stated that it is the belief of many investigators that in the case of bodies with sharp edges the vortex system is geometrically similar over the whole range of Reynolds' Numbers, except at very low values"[11].

B. RECOMMENDATIONS

Several questions arose during the course of this investigation, the answers to which were not immediately apparent. Since the element of time was an important consideration, some of the problems and peculiarities that arose are presented for reference in future investigations.

1. In order to confirm the static moment graph for section "c" it might be advisable to run a torsional motion dynamic test using springs which develop a lower frequency than those used in this test. This would allow testing in a much higher range of V/Nb for lower wind velocities.

2. A check of the static lift graph for section "d" could also be obtained by running a vertical motion dynamic test on this section with lighter springs

as described in Recommendation #1 for higher ranges of V/Nb.

3. An investigation of the variation in frequency during the dynamic tests and the correspondence of this variation with the decrement peaks, obtained in the stability response graphs themselves, might yield some qualitative results towards the solution of the forced motion aspect of the problem. The data compiled in this investigation could be used for such an investigation. Although the frequency variations for four dynamic tests were shown in this investigation, a more complete program along this line would be necessary before any definite conclusions could be drawn.

4. Direct measurement of the forces identified with the vortex effect is very desirable. As has been mentioned previously, several attempts to measure this force directly during this investigation have been unsuccessful, but in the near future it probably will be accomplished as part of the continuation of this test program.

VII. CONCLUSIONS

As a result of this investigation the following conclusions may be stated:

1. The variation in initial test amplitude for dynamic stability response tests does not change the general shape of the curve, but does affect the magnitude of the decrement in both the stable and unstable regions. An increase in initial test amplitude results in a decrease in magnitude of the decrement.

2. The opinion that the forced motion effect, identified with the Karman vortex trail, is a factor in the response graphs of bridge section models has been reinforced.

3. Section "a" is basically stable for both vertical and torsional motion. However, there is a range of non-catastrophic torsional instability which may be troublesome.

4. Section "b" is basically stable for torsional motion and basically unstable for vertical motion. As in section "a" there is also a range of non-catastrophic torsional instability which may be troublesome.

5. Section "c" is basically stable for vertical motion and catastrophically unstable for torsional

motion. There is a range of limited vertical instability which, however, has a comparatively small decrement as a maximum.

6. Section "d" is basically unstable for both vertical and torsional motion.

7. Section "e" is basically stable for torsional motion and basically unstable for vertical motion. There is a range of small limited instability for torsional motion.

Each of these five sections was carefully selected from a series of previous static tests as being basically aerodynamically stable. In each case an attempt was made to select a section which would be as close to a neutral section as possible. Yet, the results of this investigation show only one section (section "a") to be completely stable. The reason for this apparent discrepancy can be attributed only to the difference in detail between the models used for the earlier tests and the models used in these tests. This difference in detail amounted to the difference in the method of support of the girders and fins, and consequently the percentage of longitudinal openings in the deck. This illustrates the importance of details when working with essentially neutral sections. In

the cases in this investigation where the static test graphs had a negative slope, it was relatively small, but enough to indicate aerodynamic instability. Therefore, when selecting basic sections on the basis of static tests, it is advisable to choose those sections which indicate a slight positive slope of static lift and moment graphs. Adopting this policy will reduce the probability of causing the details in the actual section to shift the slope of these graphs enough to render the section unstable. This policy has been recommended previously[1] and the present investigation confirms the soundness of this procedure.

In conclusion, therefore, the selection of a final bridge section, which will be aerodynamically stable, should be based upon static tests run on basic section models. From the results of these tests, sections should be selected which have the most favorable stability characteristics, i.e., those with small positive slope of lift and moment graphs, rather than those exhibiting neutral qualities. In order to determine the magnitude and extent of possible regions of limited instability, dynamic tests should be run on actual models (with details) of the proposed sections which were selected as a

result of the static tests on the basic sections. The dynamic tests eliminate the possibility of adopting a final section which, although basically stable, might be subject to a dangerous limited instability condition which could prove disastrous if not detected.

It can, therefore, be seen that wind tunnel tests on section models offer a positive approach to the final solution of the problem of aerodynamic instability, and have been indispensable in obtaining the amount of information that is presently available on the subject.

VIII. ACKNOWLEDGMENTS

The author wishes to express his sincere appreciation and gratitude to Professor F. J. Maher for his guidance, aid and patience throughout this investigation.

The author wishes to thank Professor J. B. Eades and the V. P. I. Aeronautical Engineering Department for their help and cooperation in the use of the V. P. I. Wind Tunnel.

Acknowledgment is made to Dr. D. B. Steinman, Consulting Engineer, for suggestions regarding the selection of the most promising sections for investigation. The author also wishes to thank Dr. Steinman for the use of his correspondence with Professor Maher, pertaining to the Karman effect.

Acknowledgment is also made to the Research Corporation, of New York, N. Y., whose grant to the V. P. I. Research Foundation made this investigation possible.

IX. BIBLIOGRAPHY

1. Becker, L. A. "Aerodynamic Stability of Suspension Bridges" V.P.I. (1953) Unpublished M.S. Thesis

2. Binder, R. C. "Fluid Mechanics" Chaps. 10, 11. Prentice Hall, Inc., New York (1943)

3. Den Hartog, J. P. "Mechanical Vibrations" McGraw-Hill Book Company, Inc., New York

4. Fage, A. and Johansen, F. C. "The Flow of Air About an Inclined Flat Plate of Infinite Span" Proceedings of the Royal Society, London (1927) Vol. A116

5. Farquharson, F. B. "Aerodynamic Stability of Suspension Bridges" with reference to the Tacoma Narrows Bridge, University of Washington, Eng'g. Exp. Sta. Bul. No. 116, Part III, pp. 116-124

6. Farquharson, F. B. and Dunn, L. G. "On the Aerodynamic Investigations of a Full Model of the Original Tacoma Narrows Bridge" a Report to the Board of Consulting Engineers, November 16, 1942

7. Frazer, R. A. "Aerodynamic Oscillations of Suspension Bridges" Engineering 1951 (London, England) Vol. 171, March 2, 1951, pp. 270-271

8. Freberg and Kemler "Elements of Mechanical Vibrations" pp. 46-49 John Wiley and Sons, Inc., New York (1949)

9. Jones, B. "Elements of Practical Aerodynamics" Chaps. 1-5, 14 John Wiley and Sons, Inc., New York (1936)

10. Karman T. and Dunn, L. G. "Aerodynamic Investigation of the Bending Oscillations of the Original Tacoma Narrows Bridge" a Report to the Board of Consulting Engineers, April 12, 1943 (See Reference [5], pp. 66-73)

11. Krzywoblocki, M. A. "Investigation of the Wing-Wake Frequency with Application of the Strouhal Number" Jour. Aer. Sci., Vol. 12 (January 1945) p. 31 (See Reference [5] p. 103)

12. Maher, F. J. "Wind Tunnel Model Tests of Coosa River Pipeline Bridge" V.P.I. Eng'g. Exp. Sta. Bul. 84 (1953)

13. Maher, F. J. and Becker, L. A. "Dynamic Tests of Suspension Bridge Section Models" V.P.I. Eng'g. Exp. Sta. Bull. 98 (1955)

14. Maher, F. J., Frederick, D. and Estes, E. R. "Wind Tunnel Tests of Suspension Bridge Section Models" Part I, V.P.I. Eng'g. Exp. Sta. Bul. 69 (1948)

15. Steinman, D. B. "Design of Bridges Against Wind" Part III, Civil Eng'g. Vol. 15, 558-560 (1945)

16. Steinman, D. B. "Problems of Aerodynamic and Hydrodynamic Stability" pp. 137, Proceedings of the Third Hydraulics Conference Bulletin 31, University of Iowa Studies in Engineering (1947).

17. Steinman, D. B. "Simple Model Tests Predict Aerodynamic Characteristics of Bridges" Part II, Civil Eng'g. Vol. 17, 20-23 (1947)

18. Steinman, D. B. "Wind Tunnel Tests Yield Aerodynamically Stable Bridge Sections" Civil Eng'g (Vol. p. 746-749) December 1947

19. Steinman, D. B. "Aerodynamic Theory of Bridge Oscillations" Proceedings of Americal Society of Civil Engineers, pp. 1147-1184, October 1949

20. Steinman, D. B. Correspondence pertaining to Karman effect, dated December 8, 1954, with Professor F. J. Maher, V.P.I.

21. Steinman, D. B. Correspondence pertaining to Karman effect, dated December 4, 22, 24, 1954 with Professor F. J. Maher, V.P.I.

22. Spivak, H. M. "Vortex Frequency and Flow Pattern on the Wake of Two Parallel Cylinders at Varied Spacing Normal to an Air Stream" Jour. Aer. Sci., Vol. 13 (June 1946), p. 289

23. Thomson, W. T. "Mechanical Vibrations" p. 44 Prentice Hall, Inc., New York (1953)

The vita has been removed from the scanned document